Surface-Mediated Control of Blood Coagulation: The Role of Binding Site Densities and Platelet Deposition

Andrew L. Kuharsky* and Aaron L. Fogelson[†]

*Generation5, Toronto, Ontario, Canada; and [†]Department of Mathematics, University of Utah, Salt Lake City, Utah 84112 USA

ABSTRACT   A mathematical model of the extrinsic or tissue factor (TF) pathway of blood coagulation is formulated and results from a computational study of its behavior are presented. The model takes into account plasma-phase and surface-bound enzymes and zymogens, coagulation inhibitors, and activated and unactivated platelets. It includes both plasma-phase and membrane-phase reactions, and accounts for chemical and cellular transport by flow and diffusion, albeit in a simplified manner by assuming the existence of a thin, well-mixed fluid layer, near the surface, whose thickness depends on flow. There are three main conclusions from these studies. (i) The model system responds in a threshold manner to changes in the availability of particular surface binding sites; an increase in TF binding sites, as would occur with vascular injury, changes the system's production of thrombin dramatically. (ii) The model suggests that platelets adhering to and covering the subendothelium, rather than chemical inhibitors, may play the dominant role in blocking the activity of the TF:VIIa enzyme complex. This, in turn, suggests that a role of the IXa-tenase pathway for activating factor X to Xa is to continue factor Xa production after platelets have covered the TF:VIIa complexes on the subendothelium. (iii) The model gives a kinetic explanation of the reduced thrombin production in hemophilias A and B.

INTRODUCTION

When the wall of a blood vessel is injured, a variety of molecules that are embedded in the vessel wall become exposed to the blood, and this initiates two interacting processes known as platelet aggregation and coagulation. The first of these involves platelets, a cellular constituent of the blood. A platelet can adhere to the damaged tissue and undergo an activation process that involves changes in the platelet's surface membrane and also causes the platelet to release various chemicals into the blood plasma. The released chemicals can induce other platelets, which have not directly contacted the injured wall, to become activated and able to cohere to one another and to the already wall-adherent platelets. This is the process of platelet aggregation. Blood coagulation involves a series of enzymatic reactions, a typical one of which cleaves an inactive plasma zymogen to form an active enzyme. The initial stimulus is believed to be the formation of a particular molecular complex (tissue factor VIIa) on the injured vessel surface, and the final enzyme in the series is thrombin, which cleaves the plasma protein fibrinogen into fibrin monomers. These polymerize and cross-link to form a fibrous mesh on and between the aggregated platelets to mechanically stabilize the aggregate. Together, the platelet aggregate and fibrin mesh constitute the blood clot, and their formation comprises hemostasis, the normal response to vessel injury. These two processes are also believed to be the major

components of thrombosis, a pathological process that involves formation of a clot inside a blood vessel and that can lead to the complete occlusion of the vessel and consequent blockage of oxygen and nutrients from important organs. Understanding these processes and how they are regulated is of major medical importance. As briefly described above, platelet aggregation and coagulation may seem to be largely independent processes that only interact in the end, when the fibrin mesh forms on the platelet aggregate. In fact, there are important interactions much earlier in the processes that couple them. These include the apparently critical role played by the surface membranes of activated platelets in promoting certain coagulation reactions and the role that the coagulation enzyme thrombin plays as a potent platelet activator.

Figs. 1–3 show the major reactions of the coagulation process including interactions with platelets. As one can see from Fig. 1, coagulation involves numerous instances in which an enzyme produced in one reaction catalyzes the next reaction. It also involves feed-forward and feedback loops in which an enzyme produced in one step promotes (see Fig. 2) or inhibits (see Fig. 3) earlier or later reactions. Some of the coagulation reactions happen in the plasma, but several apparently critical reactions involve membrane-bound enzyme complexes. Despite the extreme importance of coagulation in normal hemostasis and in pathological thrombosis, people have only general (and largely unproven) ideas about what these different features may be for—the multitude of steps for signal amplification, the loops for tight regulation, the involvement of membrane-bound complexes for spatial localization. Our understanding of the dynamics of the coagulation system remains poor. The complexity of the biochemical reaction network itself, the requirement that appropriate phospholipid surfaces on activated platelets (Mann et al., 1990) be available in order
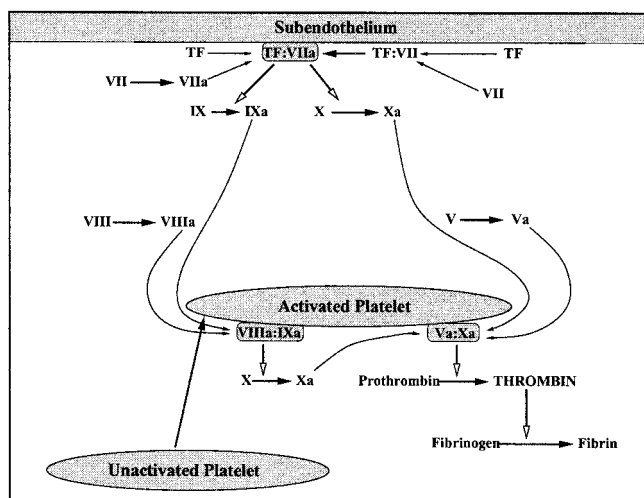
FIGURE 1 Backbone of the coagulation reaction system. Surface-bound molecular complexes (TF:VIIa on the subendothelium, and VIIIa:IXa and Va:Xa on the surface of an activated platelet) are indicated by the small rectangles. The thin arrows indicate movement of a chemical species; the thick lines with filled arrowheads indicate a molecular or cellular activation process; and the thick lines with open arrowheads depict the action of the enzymes that catalyze the activation reactions.

FIGURE 3 Chemical inhibition of coagulation. The major inhibitors (ATIII, APC, and TFPI:Xa) are indicated with small ellipses and the species affected by each inhibitor is shown by ⊣. Not shown is the postulated role of adherent platelets in physically covering TF molecules.

that the critical membrane-bound enzyme complexes can form, and the dependence on flow and diffusion (Gemmell et al., 1988) for the delivery of the chemical reactants and platelets to appropriate locations in the developing clot, all make it very difficult to synthesize a coherent picture of coagulation dynamics using traditional laboratory ap-

proaches, and make mathematical modeling a potentially very fruitful complementary tool for studying coagulation.

Below we give a brief review of the coagulation reaction system describing in words the reactions given schematically in Figs. 1–3. There are several features of the system that it is important to keep in mind. One is the presence of positive feedback loops. Another is the major role played by surface-bound enzyme complexes, and the role that regulation of the availability of binding sites for these complexes might play in the overall dynamics. A third is the role the coagulation enzymes themselves play in up-regulating the surface binding sites as well as in up-regulating inhibitors of the coagulation system.

In an earlier paper (Fogelson and Kuharsky, 1998), we investigated a simple enzyme system with membrane binding. There we saw that up-regulation of membrane binding-site density can serve as a biological switch, drastically changing the response of the system to small amounts of circulating enzyme. One goal of the current paper is to explore whether similar switch-like behavior is found in a much more comprehensive model of coagulation.

Review of the coagulation system

Coagulation is believed to be initiated when tissue factor (TF) molecules embedded in the vessel wall are exposed by injury (Nemerson, 1992) (see Fig. 1) and bind plasma enzyme factor VIIa (fVIIa). The surface-bound complex TF:VIIa activates plasma zymogens fIX and fX into enzymes fIXa and fXa (Krishnaswamy et al., 1992; Silverberg et al., 1977; Zur and Nemerson, 1980). Activated fXa in turn is a potent activator of fVII into enzyme VIIa (Radcliffe and Nemerson, 1976), particularly when fVII is al-
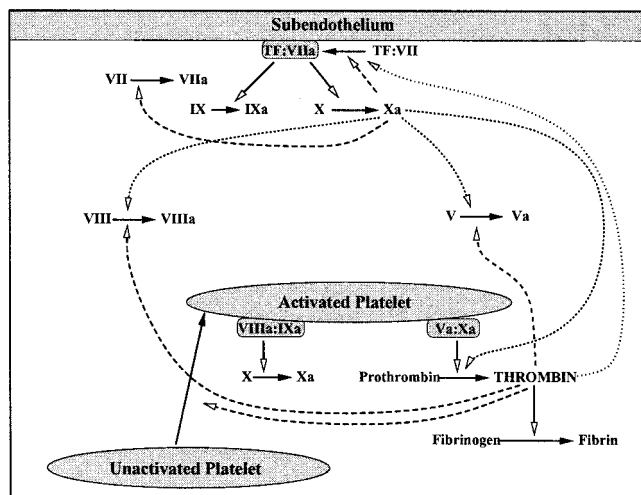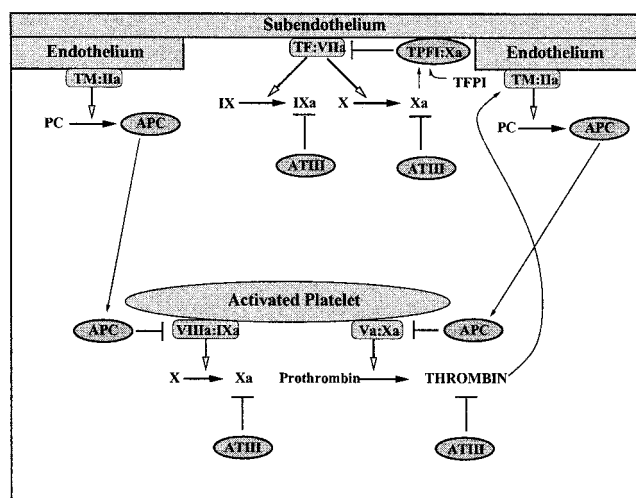

FIGURE 2 Enzymatic feedback in coagulation. The thick lines with filled arrowheads indicate a molecular or cellular activation process; the thick lines with open arrowheads indicate enzymatic activity; the dashed lines with open arrowheads indicate strong enzymatic feedback activity; and the dotted lines with open arrowheads indicate weak enzymatic feedback activity.

ready bound to TF as TF:VII (Rao and Rapaport, 1988). The TF:VIIa and fXa interaction is an example of a surface-dependent positive feedback loop. Factor Xa also activates plasma factors V and VIII into Va and VIIIa; each of these can then serve as the anchor for a membrane-bound enzyme complex (VIIIa:IXa and Va:Xa) on the surface of an activated platelet (Krishnaswamy et al., 1993; Mann et al., 1990). The platelet-bound VIIIa:IXa (tenase) complex activates X to Xa; Xa binds with Va on a platelet's surface to form the Va:Xa (prothrombinase) complex, which activates prothrombin (fII) into thrombin (fIIa). While plasma-phase fXa is a weak activator of prothrombin into thrombin (Rosing et al., 1980), the platelet-bound Va:Xa complex is a very potent thrombin activator; its effectiveness is five orders of magnitude greater (Miletich et al., 1977) than that of plasma-phase Xa and thus is likely the dominant source of thrombin activation.

The formation and activity of the VIIIa:IXa and Va:Xa complexes are critically dependent on the availability of suitable anionic phospholipid binding sites; these sites are not present on normally circulating platelets, but are present on activated platelets. Platelet activation can be induced by direct contact of platelets with collagens exposed in the injured vessel tissue, by the action of thrombin, or by other platelet-secreted plasma-phase chemical messengers like adenosine diphosphate (ADP) and thromboxane-A_2 (TXA_2).

Thrombin is the final enzyme produced by the coagulation cascade, and it plays several roles in coagulation. As mentioned above, it promotes the formation of a fibrin mesh, and this mechanically stabilizes the platelet aggregates that have formed on the injured vessel. Thrombin also promotes its own production by activating factors V and VIII and by activating platelets (Eaton et al., 1986; Monkovic and Tracy, 1990b).

Thrombin also plays at least one more, and quite different, role in coagulation. It binds with thrombomodulin (TM), which is located on the surface of the endothelial cells that line the undamaged vessel wall. This has two effects: (1) the bound thrombin is inhibited in its procoagulant role, and (2) the TM-thrombin complex activates plasma protein C into activated protein C (APC). APC is a potent anti-coagulant which cleaves factors VIIIa and Va, thus inactivating them and preventing their serving as cofactors in the VIIIa:IXa and Va:Xa complexes (Esmon, 1989). Two other major inhibitors of coagulation are antithrombin III (ATIII) and tissue factor pathway inhibitor (TFPI). ATIII competitively inhibits thrombin and factors IXa and Xa (Bauer and Rosenberg, 1987), whereas TFPI binds with fXa to inhibit the activity of the TF:VIIa complex (Broze et al., 1990; Rapaport, 1989) and to block the activity of the fXa that is bound to TFPI. Excellent reviews of the coagulation pathways can be found in Hemker and Kessels (1991), Jesty and Nemerson (1995), and Mann et al. (1990).

Previous models

Nesheim and coworkers (Nesheim et al., 1984, 1992) explored a steady-state model of prothrombinase activity which involves two phases, one corresponding to the bulk solution, and the other to thin shells surrounding phospholipid membranes. More recent modeling from the same laboratory (Jones and Mann, 1994) looked at dynamic interactions among a number of the coagulation enzymes and zymogens. These new models ignored inhibition and, importantly, assumed a great excess of phospholipid, and therefore did not address the possible regulatory role played by phospholipid surfaces in controlling the coagulation reactions. Willems et al. (1991) studied a dynamic model of thrombin production in plasma, allowing for inhibition by APC and exogenous hirudin. The stimulus in the system is a brief pulse of fXa, and a threshold response to this stimulus was reported. The model inputs included phospholipid concentration, but the effect of this concentration on system behavior was not reported. Baldwin and Basmadjian (1994) modeled the part of the coagulation network that includes activation of zymogens fX and prothrombin, feedback activation of cofactors fV and fVIII by thrombin, and degradation of fXa and thrombin due to inhibitors. Their model includes transport of chemical species to/from a surface consisting of the membranes of platelets assumed to be adherent to the vessel wall. This membrane is assumed to be present in large excess. TF:VIIa activation of fX and fIX are not included, and instead exogenous fIXa is introduced. The main results of the paper are (i) the existence of multiple steady-state solutions at intermediate levels of mass transport, and (ii) dynamic results that indicate very slow development of thrombin at low mass-transfer rates, very little development of thrombin at high mass-transfer rates, and, depending on the initial concentration of thrombin, little or substantial production of thrombin over periods relevant for hemostasis, at intermediate mass-transfer rates. Jesty et al. (1993) analyzed a simple system which involves two zymogen-enzyme pairs in a positive feedback loop with inhibition. In their system, each zymogen is activated by the enzyme of the other zymogen-enzyme pair, and both enzymes are subject to first-order inactivation. Their main result was that the system has a threshold. If the product of activation rates is less than the product of inactivation rates, then the system's response to a stimulus (an increment of enzyme) quickly decays. If the product of activation rates exceeds the product of inactivation rates, the same stimulus produces a large conversion of zymogen to enzyme. Beltrami and Jesty (1995) extended this analysis to larger systems made up of multiple interacting feedback loops. These results are interesting but limited because the analysis is for solution-phase reactions only; no account is taken of surface binding or transport of reactants to and from reactive surfaces, even though surface reactions seem to play a major regulatory role in coagulation. In earlier work (Fo-

gelson and Kuharsky, 1998), we considered an extension of the Jesty-Beltrami approach, which includes both solution-phase and membrane-phase reactions, and in which the concentrations of membrane binding-sites are limited and treated as control variables. As mentioned above, we found that up-regulation of membrane binding-site density can serve as a biological switch modulating the threshold value of the system, and changing the status of the system from 'off' (in which even large amounts of circulating enzyme produce only a transient decaying response) to 'on' (in which even small amounts of circulating enzyme produce a large and sustained response). This result holds when the preponderance of enzymatic activity is vested in the membrane-bound enzymes, as seems to be the case in coagulation. It holds in models in which the two phases are assumed to be well mixed (as in the limit of very fast diffusion) and in models in which there is diffusion at physiological rates between the solution and membrane phases.

In the current paper we look at a much more comprehensive model of coagulation biochemistry that also takes into account, in a simplified way, the effect of transport of chemicals and platelets and the competing effects of activated platelets in providing pro-coagulant surfaces and in covering the exposed injury by adhering to it.

MODEL ASSUMPTIONS

In this section, we describe a mathematical model of the tissue factor pathway of blood coagulation that takes into account plasma-phase and phospholipid-membrane-bound enzymes and zymogens, coagulation inhibitors, and activated and unactivated platelets. The model includes both plasma-phase and membrane-phase reactions. We consider events that occur after exposure of an area of subendothelium of axial length L and circumferential width W on the surface of a vessel of radius R. We assume that all reactions of interest occur in a thin boundary layer shell above the injured surface. We assume that all species (plasma-phase and membrane-phase) in this shell are well mixed, and it follows from this assumption that all reactions can be described using ordinary differential equations in time.

Initially the shell is filled only with fluid and chemicals, and has a thickness determined by the relative influence of zymogen transport by radial diffusion and axial convection. For the situations considered in this paper, this chemical boundary layer thickness ranges from 0.4 to 2.0 μm. As time progresses, platelets enter the region and adhere to the subendothelium or aggregate on already adherent platelets, and this increases the total thickness and volume of the shell.

Flow and diffusion combine to bring proteins into the shell from upstream and to carry them downstream, away from the damaged wall. These effects are incorporated into the model in a simple way by assuming that each plasma-phase protein is delivered to or removed from the shell at a rate proportional to the difference between its concentration within the shell and its concentration far outside of the shell. Hence, the equations that describe how the concentrations of plasma-phase proteins change with time involve terms of the form $k_{flow}^c (c^{out} - c)$ where c is the concentration within the shell, c^{out} is the concentration far outside of the shell, and k_{flow}^c denotes the rate function. The value of k_{flow}^c depends on flow and diffusion parameters and on other factors described in Appendix A.

Unactivated platelets are also transported by flow and diffusion, and, in addition, can undergo an activation process and can adhere to the damaged vessel wall and to other adherent platelets. The equation that governs how the concentration of unactivated platelets changes with time involves a term $k_{flow}^p ([PL]^{out} - [PL])$ with $[PL]$ and $[PL]^{out}$ the concentrations of unactivated platelets in and outside of the boundary layer, respectively. The rate function k_{flow}^p for platelet transport has a different value than that for zymogen and enzyme transport. This is because we take the platelet boundary layer thickness to be 2–3 μm, the distance over which platelets can attach to one another because of their pseudopodia (Frojmovic et al., 1990), and this is greater than the thickness of the zymogen/enzyme chemical boundary layer as determined from the protein's Peclet number. Note that the units of k_{flow}^c and k_{flow}^p are s^{-1}. This differs from mass-transfer coefficients often used in the engineering literature (see, for example, Baldwin and Basmadjian (1994); Cussler (1984)) where the mass transfer coefficient k has units of cm/s. The reason for the difference is that k_{flow}^c $(c^{out} - c)$ describes transport into the volume of the shell, whereas in the references cited, $k(c^{out} - c)$ describes transport to a surface. Further discussion of the relationship between our k_{flow}^c and the mass-transfer coefficient k is given in Appendix A.

Assumptions about platelets

Three different populations of platelets are considered in the model: (i) unactivated and free in solution, (ii) activated and attached directly to the subendothelium, and (iii) activated but not attached directly to the subendothelium. Only the unactivated platelets are treated as free to move out of the shell because of the flow; we think of the activated platelets in the shell that are not attached directly to the subendothelium as part of a wall-bound aggregate. Unactivated platelets can become activated in three ways: (i) by directly reacting with the subendothelium and binding to it, (ii) by exposure to sufficiently high concentrations of the coagulation enzyme thrombin, and (iii) by exposure to other already activated platelets. The last mechanism is used as a surrogate for platelet activation by chemicals (e.g., ADP) secreted by platelets but not explicitly included in the model. The two populations of activated platelets provide binding sites with which some of the coagulation zymogens and enzymes can react. In taking into account the role of the activated platelets in the coagulation reactions, we regard them as uniformly distributed over the volume of the shell. For other purposes, it is useful to think of the activated platelets as stacked in layers. We regard each wall-adherent platelet as covering a specified area of the exposed subendothelium. To compute the current number of layers, we calculate the number of activated platelets in the shell (the concentration of activated platelets times the shell volume) and divide this by the maximum number of platelets that can directly bind to the subendothelium (the subendothelial area $L \cdot W$ divided by the area covered by a single platelet). Each successive platelet layer increases the size of the shell and the volume in which the chemicals interact. This volume consists of the chemical boundary layer above the platelet layers and the spaces between platelets within the layers. Because the part of this volume between the adherent platelets is relatively sheltered from the flow, the overall rate of flow-mediated delivery of zymogen to the shell or flow-mediated removal of enzyme from the shell decreases as the number of platelet layers increases. This is reflected in a reduction in the parameters k_{flow}^c and k_{flow}^p from their initial values by a factor equal to the current ratio of volume in the chemical boundary layer to the volume in the chemical boundary layer and in the spaces between the platelets. Because the model does not provide for shear-induced removal of platelets as a mechanism for limiting aggregate size, we explicitly limit the number of platelet layers that are allowed to form, usually to four or fewer.

Assumptions about reactants

1. Factors VII and VIIa can bind to TF on the exposed subendothelium (Radcliffe and Nemerson, 1976). Factor Xa activates factor VII in plasma as well as when factor VII is bound to TF (Radcliffe and Nemerson, 1975). We assume that Xa binds to the TF:VII complex directly from plasma without having to first bind to the subendothelium.

2. Factors IX and X can be activated to IXa and Xa respectively by the TF:VIIa complex on the subendothelium (Zur and Nemerson, 1980; Silverberg et al., 1977). This is the only source of factor IXa. Factor X can also be activated by the VIIIa:IXa (tenase) complex on the surface of an activated platelet. Factors X and IX are assumed to attach to TF:VIIa directly from plasma.

3. Factors V and VIII can be activated to factors Va and VIIIa by thrombin in plasma and by thrombin and factor Xa on the surfaces of activated platelets (Vehar and Davie, 1980; Monkovic and Tracy, 1990b).

4. The inhibitors of the coagulation reactions that we include in the model are antithrombin III (ATIII), activated protein C (APC), and tissue factor pathway inhibitor (TFPI). Since the concentration of ATIII is very high in plasma, we assume it acts in a first-order manner to inactivate plasma factors IXa, Xa, and thrombin. APC is assumed to bind directly from solution to platelet-bound factors Va and VIIIa and to permanently inactivate them (Solymoss et al., 1988; Walker et al., 1987) with second-order kinetics. Because APC is produced by a complex of thrombin and thrombomodulin (TM) on healthy endothelial cells near the damaged wall, we regard the concentration of APC as a function of the quantity of thrombin that has left the shell. To account for the time it takes thrombin to leave the shell, bind to TM, and activate protein C, and the time for APC to enter the shell, we assume that there is a lag t_{lag} and that the APC level at time t depends on the thrombin level at time $t - t_{lag}$. TFPI must first bind to factor Xa, and then the complex TFPI:Xa binds to the TF:VIIa complex and inhibits it (Broze et al., 1988).

Assumptions about the binding of proteins to surfaces

1. Factors VII and VIIa compete for the TF binding sites on the subendothelium.

2. Factors IX and X compete for the TF:VIIa complex on the subendothelium.

3. Each zymogen/enzyme pair, II/IIa, V/Va, VIII/VIIIa, and X/Xa has distinct binding sites on activated platelets for which the zymogen and enzyme compete. For IX/IXa, we consider two scenarios: one in which IX/IXa compete for binding sites, and one in which there is also a set of binding sites for IXa alone (Ahmad et al., 1989). We refer to these as shared and IXa-specific binding sites, respectively.

Our model includes the possibility that the activity of the TF:VIIa complex decreases as platelet deposition on the injured tissue increases. That is, we allow for the possibility that as platelets cover the exposed subendothelium, they physically block the activity of the TF:VIIa complex. This has important consequences regarding the behavior of the model system and the experiments and reasoning that led us to include this possibility are discussed below.

Notation

The coagulation reactions we consider are listed in Tables 1–6. Z_i and E_i refer to zymogen i and enzyme i in solution, and Z_i^m and E_i^m refer to the membrane-bound versions of these proteins (e.g., E_7^m refers to the TF:VIIa complex and E_5^m refers to fVa bound to the platelet surface). Concentrations are denoted in a similar way but with lower-case z and e. TF, P_2, P_5, P_8, P_9, and P_{10} refer to tissue factor and the binding sites on activated platelets for prothrombin/thrombin and factors V/Va, VIII/VIIIa, IX/IXa, and X/Xa, respectively; $[TF]$, p_2, p_5, p_8, p_9, and p_{10} refer to the concentrations of these binding sites; and N_5^{pl}, N_{10}^{pl}, N_8^{pl}, N_9^{pl}, and N_2^{pl} refer to the number of these receptors expressed on the surface of a platelet when the platelet is activated. Quantities pertaining to the IXa-specific binding sites are denoted in a similar way but with an additional superscript *, e.g., p_9^* is the concentration of IXa-specific sites, and $e_9^{m,*}$ is the concentration of IXa bound to these sites. We denote a complex of Z_i and E_j by $Z_i:E_j$ and its concentration by $[Z_i:E_j]$. Special symbols are used for the platelet-bound tenase VIIIa:IXa and prothrombinase Va:Xa complexes, $TEN =$ VIIIa:IXa and $PRO =$ Va:Xa; $[TEN]$ and $[PRO]$ denote their respective concentrations. Unactivated platelets are denoted by PL; activated platelets attached to the subendothelium by PL_a^s; and activated platelets not attached to the subendothelium by PL_a^v. The respective platelet concentrations are $[PL]$, $[PL_a^s]$, and $[PL_a^v]$. The inhibitors are denoted APC and $TFPI$ with concentrations $[APC]$ and $[TFPI]$. The full set of model equations is listed in Appendix B. In the following paragraphs, we use several of the equations to explain the different types of terms that appear in the full set of equations.

Terms in the model equations

Equation 4 in Appendix B is:

$$\frac{de_2^m}{dt} = k_2^{on} c_2 (p_2 - z_2^{mtot} - e_2^{mtot})$$

$$- k_2^{off} e_2^m + k_7^{cat} [Z_2^m : PRO]$$

$$+ (k_{13}^{cat} + k_{13}^-)[Z_5^m : E_2^m] - k_{13}^+ z_5^m e_2^m$$

$$+ (k_{15}^{cat} + k_{15}^-)[Z_8^m : E_2^m] - k_{15}^+ z_8^m e_2^m$$

Here, the term $k_2^{on} e_2 (p_2 - z_2^{mtot} - e_2^{mtot})$ gives the rate at which the plasma-phase enzyme E_2 (thrombin) binds to the surface of an activated platelet; p_2 is the total volume concentration of binding sites for Z_2 and E_2 on the activated platelets in the shell, from which the concentration of occupied binding sites $z_2^{mtot} + e_2^{mtot}$ is subtracted to give the concentration of unoccupied sites. The quantities z_2^{mtot} and e_2^{mtot} denote the concentrations

TABLE 1 Reactions on subendothelium

Reaction	Reactants	Complex	Product	M^{-1} s^{-1}	s^{-1}	s^{-1}	Note
VII binding with TF	Z_7, TF		Z_7^m	$k_7^{on} = 5.0 \cdot 10^7$	$k_7^{off} = 5.0 \cdot 10^{-3}$		a
VIIa binding with TF	E_7, TF		E_7^m	$k_7^{on} = 5.0 \cdot 10^7$	$k_7^{off} = 5.0 \cdot 10^{-3}$		a
Xa activation of TF:VII	E_{10}, Z_7^m	$Z_7^m:E_{10}$	E_7^m	$k_2^+ = 5.0 \cdot 10^6$	$k_2^- = 1.0$	$k_2^{cat} = 5.0$	b
IIa activation of TF:VII	E_2, Z_7^m	$Z_7^m:E_2$	E_7^m	$k_3^+ = 3.92 \cdot 10^5$	$k_3^- = 1.0$	$k_3^{cat} = 6.1 \cdot 10^{-2}$	c
TF:VIIa activation of X	E_7^m, Z_{10}	$Z_{10}:E_7^m$	E_{10}	$k_8^+ = 8.95 \cdot 10^6$	$k_8^- = 1.0$	$k_8^{cat} = 1.15$	d
TF:VIIa activation of IX	E_7^m, Z_9	$Z_9:E_7^m$	E_9	$k_9^+ = 8.95 \cdot 10^6$	$k_9^- = 1.0$	$k_9^{cat} = 1.15$	e

(a) $K_d = 1.0 \cdot 10^{-10}$ M (Nemerson, 1992).
(b) $k_2^{cat} = 5.0$ s^{-1} and $K_M = 1.2 \cdot 10^{-6}$ M (Butenas and Mann, 1996).
(c) $k_3^{cat} = 6.1 \cdot 10^{-2}$ s^{-1} and $K_M = 2.7 \cdot 10^{-6}$ M (Butenas and Mann, 1996).
(d) $k_8^{cat} = 1.15$ s^{-1} and $K_M = 4.5 \cdot 10^{-7}$ M (Mann et al., 1990).
(e) We assume that the reaction constants for TF:VIIa activation of fIX are the same as for TF:VIIa activation of fX.

TABLE 2 Reactions in the plasma

Reaction	Reactants	Complex	Product	M^{-1} s^{-1}	s^{-1}	s^{-1}	Note
Xa activation of VII	Z_7, E_{10}	$Z_7{:}E_{10}$	E_7	$k_1^+ = 5 \cdot 10^6$	$k_1^- = 1.0$	$k_1^{cat} = 5.0$	a
IIa activation of VII	Z_7, E_2	$Z_7{:}E_2$	E_7	$k_{18}^+ = 3.92 \cdot 10^5$	$k_{18}^- = 1.0$	$k_{18}^{cat} = 6.1 \cdot 10^{-2}$	b
IIa activation of V	Z_5, E_2	$Z_5{:}E_2$	E_5	$k_{12}^+ = 1.73 \cdot 10^7$	$k_{12}^- = 1.0$	$k_{12}^{cat} = 0.23$	c
IIa activation of VIII	Z_8, E_2	$Z_8{:}E_2$	E_8	$k_{14}^+ = 2.64 \cdot 10^7$	$k_{14}^- = 1.0$	$k_{14}^{cat} = 0.9$	d

(a) $k_1^{cat} = 5.0$ s^{-1} and $K_M = 1.2 \cdot 10^{-6}$ M (Butenas and Mann, 1996).
(b) $k_{18}^{cat} = 6.1 \cdot 10^{-2}$ s^{-1} and $K_M = 2.7 \cdot 10^{-6}$ M (Butenas and Mann, 1996).
(c) $k_{12}^{cat} = 0.23$ s^{-1} and $K_M = 7.17 \cdot 10^{-8}$ M (Monkovic and Tracy, 1990b).
(d) $k_{14}^{cat} = 0.9$ s^{-1} (Hill-Eubanks and Lollar, 1990) and $K_M = 2 \cdot 10^{-7}$ M (Lollar et al., 1985).

of platelet-bound prothrombin and thrombin, respectively, along with their platelet-bound complexes, so $z_2^{mtot} = z_2^m + [Z_2^m{:}PRO]$ and $e_2^{mtot} = e_2^m + [Z_5^m{:}E_2^m] + [Z_8^m{:}E_2^m]$. The term $k_2^{off} e_2^m$ is the rate of dissociation of thrombin from the platelet surface. The terms $(k_{13}^{cat} + k_{13}^-) [Z_5^m{:}E_2^m]$ and $-k_{13}^+ z_5^m e_2^m$ pertain to the association/dissociation of Z_5^m with E_2^m on the platelet surface and the enzymatic activation of Z_5^m to E_5^m. The terms $(k_{15}^{cat} + k_{15}^-) [Z_8^m{:}E_2^m] - k_{15}^+ z_8^m$ play a similar role in describing the interactions of thrombin with platelet-bound Z_8^m.

The new types of terms in Eq. 5:

$$\frac{dz_5}{dt} = -k_5^{on} z_5(p_5 - z_5^{mtot} - e_5^{mtot}) + k_5^{off} z_5^m$$

$$- k_{12}^+ z_5 e_2 + k_{12}^-[Z_5{:}E_2]$$

$$+ N_5 \frac{d([PL_a^s] + [PL_a^v])}{dt} - k_{flow}^c(z_5^{out} - z_5)$$

include $k_{12}^+ z_5 e_2$, which is the rate at which plasma-phase fV and plasma-phase thrombin bind to form the $Z_5{:}E_2$ complex, and $k_{12}^-[Z_5{:}E_2]$, which is the rate at which this complex dissociates. The term $N_5 d([PL_a^s] + [PL_a^v])/dt$ gives the rate of appearance of fV due to its release by platelets upon activation. The final term, $k_{flow}^c (z_5^{out} - z_5)$, describes the transport of fV into the shell by flow and diffusion.

Equation 49

$$\frac{d[PL_a^v]}{dt} = -k_{pla}^+(p_{sub} - [PL_a^s])[PL_a^v]$$

$$+ k_{pla}^-[PL_a^s] + k_{c_2}^{act}[PL]A(e_2)$$

$$+ k_{pla}^{act}([PL_a^s] + [PL_a^v])[PL],$$

describes the rate at which the concentration of activated platelets not attached to the subendothelium changes. The term $-k_{pla}^+ (p_{sub} - [PL_a^s])[PL_a^v]$ is the rate of deposition of activated platelets onto the subendothelium; $(p_{sub} - [PL_a^s])$ is the concentration of available platelet binding sites on the subendothelium and k_{pla}^+ is the second-order rate constant for deposition. The term $k_{pla}^-[PL_a^s]$ describes platelet detachment from the subendothelium. The term $k_{c_2}^{act} [PL] A(e_2)$ describes irreversible activation of unactivated platelets by thrombin at a rate which depends on the thrombin concentration. We have experimented with different choices of the function $A(e_2)$, using either $A(e_2) = e_2/(e_2^{pla} + e_2)$ or $A(e_2) = H(e_2 - e_2^{pla})$ with very little difference in results. Here, e_2^{pla} is a prescribed level of thrombin concentration (e.g., 1 nM) characteristic of the thrombin concentrations that affect platelets, and $H(x)$ is the step function, which has value 0 for all $x < 0$ and value 1 for all $x > 0$. For the simulations reported in this paper, we used the first version of $A(e_2)$. The final term, $k_{pla}^{act}([PL_a^s] +$

TABLE 3 Binding to platelet surfaces

Reaction	Reactants	Products	M^{-1} s^{-1}	s^{-1}	Note
Factors IX	Z_9, P_9	Z_9^m	$k_9^{on} = 1.0 \cdot 10^7$	$k_9^{off} = 2.5 \cdot 10^{-2}$	a
Factors IXa	E_9, P_9	E_9^m	$k_9^{on} = 1.0 \cdot 10^7$	$k_9^{off} = 2.5 \cdot 10^{-2}$	a
Factors IXa	E_9, P_9^*	$E_9^{m,*}$	$k_9^{on} = 1.0 \cdot 10^7$	$k_9^{off} = 2.5 \cdot 10^{-2}$	b
Factors X	Z_{10}, P_{10}	Z_{10}^m	$k_{10}^{on} = 1.0 \cdot 10^7$	$k_{10}^{off} = 2.5 \cdot 10^{-2}$	a
Factors Xa	E_{10}, P_{10}	E_{10}^m	$k_{10}^{on} = 1.0 \cdot 10^7$	$k_{10}^{off} = 2.5 \cdot 10^{-2}$	a
Factors V	Z_5, P_5	Z_5^m	$k_5^{on} = 5.7 \cdot 10^7$	$k_5^{off} = 0.17$	c
Factors Va	E_5, P_5	E_5^m	$k_5^{on} = 5.7 \cdot 10^7$	$k_5^{off} = 0.17$	c
Factors VIII	Z_8, P_8	Z_8^m	$k_8^{on} = 5.0 \cdot 10^7$	$k_8^{off} = 0.17$	d
Factors VIIIa	E_8, P_8	E_8^m	$k_8^{on} = 5.0 \cdot 10^7$	$k_8^{off} = 0.17$	d
Factors II	Z_2, P_2	Z_2^m	$k_2^{on} = 1.0 \cdot 10^7$	$k_2^{off} = 5.9$	e
Factors IIa	E_2, P_2	E_2	$k_2^{on} = 1.0 \cdot 10^7$	$k_2^{off} = 5.9$	e

(a) For fIX binding to platelets, $K_d = 2.5 \cdot 10^{-9}$ M (Ahmad et al., 1989), and for fX binding to platelets, K_d has approximately the same value (Walsh, 1994). For fX binding to PCPS vesicles, the on-rate is about 10^7 M^{-1} s^{-1} and the off-rate is about 1.0 s^{-1} (Krishnaswamy et al., 1988), giving a dissociation constant of about 10^{-7} M. To estimate on- and off-rates for the higher-affinity binding of fX to platelets, we keep the on-rate the same as for vesicles and adjust the off-rate to give the correct dissociation constant. The rates for fIX binding with platelets are taken to be the same as for fX binding.
(b) We assume binding constants for fIXa binding to the specific fIXa binding sites are the same as for shared sites.
(c) fV binds with high-affinity to phospholipids (PCPS) (Krishnaswamy et al., 1988) and we use the same rate constants reported there to describe fV binding to platelets.
(d) The K_d for fVIII binding with platelets is taken from (Nesheim et al., 1988). We set the off-rate k_8^{off} for fVIII binding to platelets equal to that for fV binding to platelets, and calculate the on-rate k_8^{on}.
(e) For prothrombin interactions with platelets, K_d is reported to be $5.9 \cdot 10^{-7}$ M (Mann, 1994). We choose k_2^{off} and set $k_2^{on} = k_2^{off}/K_d$.

TABLE 4 Reactions on platelet surfaces

Reaction	Reactants	Complex	Product	M^{-1} s^{-1}	s^{-1}	s^{-1}	Note
Xa activation of V	Z_5^m, E_{10}^m	$Z_5^m:E_{10}^m$	E_5^m	$k_5^+ = 1.0 \cdot 10^8$	$k_5^- = 1.0$	$k_5^{cat} = 4.6 \cdot 10^{-2}$	a
IIa activation of V	Z_5^m, E_2^m	$Z_5^m:E_2^m$	E_5^m	$k_{13}^+ = 1.73 \cdot 10^7$	$k_{13}^- = 1.0$	$k_{13}^{cat} = 0.23$	b
Xa activation of VIII	Z_8^m, E_{10}^m	$Z_8^m:E_{10}^m$	E_8^m	$k_6^+ = 5.1 \cdot 10^7$	$k_6^- = 1.0$	$k_6^{cat} = 2.3 \cdot 10^{-2}$	c
IIa activation of VIII	Z_8^m, E_2^m	$Z_8^m:E_2^m$	E_8^m	$k_{15}^+ = 2.64 \cdot 10^7$	$k_{15}^- = 1.0$	$k_{15}^{cat} = 0.9$	d
VIIIa binding with IXa	E_8^m, E_9^m		TEN	$k_{ten}^+ = 1.0 \cdot 10^8$	$k_{ten}^- = 0.01$		e
VIIIa binding with IXa*	$E_8^m, E_9^{m,*}$		TEN^*	$k_{ten}^+ = 1.0 \cdot 10^8$	$k_{ten}^- = 0.01$		e
Va binding with Xa	E_5^m, E_{10}^m		PRO	$k_{pro}^+ = 1.0 \cdot 10^8$	$k_{pro}^- = 0.01$		e
VIIIa:IXa activation of X	Z_{10}^m, TEN	$Z_{10}^m:TEN$	E_{10}^m	$k_4^+ = 1.31 \cdot 10^8$	$k_4^- = 1.0$	$k_4^{cat} = 20.0$	f
VIIIa:IXa* activation of X	Z_{10}^m, TEN^*	$Z_{10}^m:TEN^*$	E_{10}^m	$k_4^+ = 1.31 \cdot 10^8$	$k_4^- = 1.0$	$k_4^{cat} = 20.0$	f
Va:Xa activation of II	Z_2^m, PRO	$Z_2^m:PRO$	E_2^m	$k_7^+ = 1.03 \cdot 10^8$	$k_7^- = 1.0$	$k_7^{cat} = 30.0$	g

(a) $k_5^{cat} = 0.046$ s^{-1} and $K_M = 10.4 \cdot 10^{-9}$ M (Monkovic and Tracy, 1990a).
(b) The rate constants for thrombin activation of fV on platelets are assumed to be the same as in plasma.
(c) $k_6^{cat} = 0.023$ s^{-1} and $K_M = 2.0 \cdot 10^{-8}$ M (Lollar et al., 1985).
(d) The rate constants for thrombin activation of fVIII on platelets are assumed to be the same as in plasma.
(e) The formation of the tenase and prothrombinase complexes is assumed to be very fast with $K_d = 1.0 \cdot 10^{-10}$ M (Mann, 1987).
(f) $k_4^{cat} = 20$ s^{-1} and $K_M = 1.6 \cdot 10^{-7}$ M (Rawala-Sheikh et al., 1990).
(g) $k_7^{cat} = 30$ s^{-1} and $K_M = 3.0 \cdot 10^{-7}$ M (Nesheim et al., 1992).

$[PL_a^v])[PL]$ corresponds to the activation of unactivated platelets through contact with activated platelets. As noted before, we regard this activation mechanism as a surrogate for activation by platelet-released agonists such as ADP and TXA$_2$.

In Eq. 12,

$$\frac{de_7^m}{dt} = k_7^{on}e_7([TF] - e_7^{mtot} - z_7^{mtot}) - k_7^{off}e_7^m$$

$$+ k_2^{cat}[Z_7^m:E_{10}] + k_3^{cat}[Z_7^m:E_2]$$

$$+ (k_8^- + k_8^{cat})[Z_{10}:E_7^m] - k_8^+ z_{10}e_7^m$$

$$+ (k_9^- + k_9^{cat})[Z_9:E_7^m] - k_9^+ z_9 e_7^m$$

$$- k_{11}^+[TFPI:E_{10}]e_7^m$$

$$+ k_{11}^-[TFPI:E_{10}:E_7^m] - e_7^m\frac{p'}{1-p}$$

the variable p is the fraction of the subendothelial surface area covered by platelets ($p = [PL_a^s]/p_{sub}$), p' is the rate of change of p; and the expression $-p'/(1 - p) = (1 - p)'/(1 - p)$ is the fractional rate of change of uncovered subendothelial area. The last term in the equation says that the concentration of TF:VIIa decreases at a fractional rate equal to the frac-

tional rate of decrease of uncovered subendothelial area. This term embodies our assumption that as platelets bind to the subendothelium the number of TF molecules (and complexes involving TF) available to participate in the coagulation process decreases and therefore the concentration of available TF molecules in the shell also decreases. A similar term appears in each equation for a species that involves TF.

Parameter evaluation

To do simulations with the model system, we must specify values of the kinetic parameters, initial concentrations for all species, and the upstream concentration (i.e., the concentration outside of the shell) for all plasma-phase species. For zymogens, the initial and upstream concentrations are set to their normal plasma concentrations. All enzyme and complex concentrations are initially set to zero except for the concentration of fVIIa (e_7), which is set to 1% of the normal fVII concentration. Typical values of these parameters are given in Tables 1–7. In some simulations different values are used, and this is indicated in the description of those simulations.

It is typical for enzymatic reactions that literature values are available for the Michaelis-Menton parameter $K_M = (k^- + k^{cat})/k^+$ and the turnover number k^{cat} but not for k^- and k^+ separately. In this situation, we choose a value for k^- in the range (0.1–10.0 s^{-1}) in which most known enzyme reverse rates lie, and then calculate the corresponding $k^+ = (k^- + k^{cat})/K_M$. Similarly, for binding reactions, the dissociation constant $K_d = k^{off}/k^{on}$ is often available, whereas the separate on- and off-rates k^{on} and k^{off} are not. Again, we choose a value for k^{off} (usually 1.0) and compute the corre-

TABLE 5 Inhibition reactions

Reaction	Reactants	Complex	Product	M^{-1} s^{-1}	s^{-1}	s^{-1}	Note
APC inactivation of VIIIa	APC, E_8^m	$APC:E_8^m$	$E_8^{m,in}$	$k_{17}^+ = 1.2 \cdot 10^8$	$k_{17}^- = 1.0$	$k_{17}^{cat} = 0.5$	a
APC inactivation of Va	APC, E_5^m	$APC:E_5^m$	$E_5^{m,in}$	$k_{16}^+ = 1.2 \cdot 10^8$	$k_{16}^- = 1.0$	$k_{16}^{cat} = 0.5$	a
TFPI binding with Xa	$TFPI, E_{10}$		$TFPI:E_{10}$	$k_{10}^+ = 1.6 \cdot 10^7$	$k_{10}^- = 3.3 \cdot 10^{-4}$		b
TFPI:Xa binding with TF:VIIa	$TFPI:E_{10}$ E_7^m		$TFPI:E_{10}:E_7^m$	$k_{11}^+ = 1.0 \cdot 10^7$	$k_{11}^- = 1.1 \cdot 10^{-3}$		b
ATIII inactivation of IXa	E_9		E_9^{in}		$k_9^{in} = 0.1$		c
ATIII inactivation of Xa	E_{10}		E_{10}^{in}		$k_{10}^{in} = 0.1$		c
ATIII inactivation of IIa	E_2		E_2^{in}		$k_2^{in} = 0.2$		c

(a) For inhibition of fVa by APC, $k_{16}^{cat} = 0.45$ s^{-1} and $K_M = 12.5 \cdot 10^{-9}$ M (Solymoss et al., 1988). We assume the same reaction rates for the inhibition of fVIIIa by APC.
(b) From Jesty et al. (1994).
(c) We estimate these parameters based on the half-lives of factors IXa, Xa, IIa in plasma (Rosenberg and Bauer, 1994).

TABLE 6 Platelet responses

Reaction	Reactants	Products	M^{-1} s^{-1}	s^{-1}	Note
Unactivated platelet binding to SE	PL, P_{sub}	PL_a^s	$k_{pla}^+ = 2 \cdot 10^{10}$	$k_{pla}^- = 0.0$	a
Activated platelet binding to SE	PL_a^v, P_{sub}	PL_a^s	$k_{pla}^+ = 2 \cdot 10^{10}$	$k_{pla}^- = 0.0$	a
Platelet activation by platelet in solution	PL, PL_a^v	$2\ PL_a^v$	$k_{pla}^{act} = 3 \cdot 10^8$		b
Platelet activation by platelet on SE	PL, PL_a^s	PL_a^v, PL_a^s	$k_{pla}^{act} = 3 \cdot 10^8$		b
Platelet activation by thrombin	PL, E_2	PL_a^v		$k_{c_2}^{act} \cdot A(e_2) = 0.50$	b

(a) Estimated from data in Turitto and Baumgartner (1979) and Turitto et al. (1980) as described in text.
(b) Estimated from data in Gear (1994) as described in text.

sponding $k^{on} = k^{off}/K_d$. We set k^{off} to a smaller value, if necessary, to keep k^{on} from exceeding the diffusion-limited rate of about 10^8 M^{-1} s^{-1}.

We model platelet deposition as a second-order reaction between platelets and binding sites on the subendothelium, and estimate the rate constant k_{pla}^+ for this reaction from experimental data. Although we have found no data for platelet deposition on subendothelial regions of the small size we consider, we can extract estimates of the deposition rate from macroscopic-scale studies such as Turitto and Baumgartner (1979) and Turitto et al. (1980). In these studies, the percent of surface coverage was measured for a number of thin vessel sections at distances x between 3.5 and 10 mm from the upstream end of the exposed subendothelium. The average of these measurements was computed for times ranging from 1 to 40 min, and initial rates of deposition were also calculated. These initial rates are unlikely to be confounded by effects on adhesion of upstream thrombus growth, and so give cleaner data for our purposes here. The same papers present theoretical formulas in which the deposition rate decreases with axial distance according to the power law $x^{-1/3}$. We use this power law to extrapolate the measured deposition rates at $x \approx 5$–10 mm to the position $x = 10\ \mu$m relevant for our simulations, and then use these extrapolated rates to estimate the time needed for 95% of our small subendothelial region to be covered. We find that these times fall in the range 3–5 min, compared to times of 30–40 min at the far downstream locations at which

TABLE 7 Normal concentrations and surface binding site numbers

Prothrombin: z_2^{out}	1.4 μM	a
Factor V: z_5^{out}	0.01 μM	b
Factor VII: z_7^{out}	0.01 μM	a
Factor VIIa: e_7^{out}	0.1 nM	c
Factor VIII: z_8^{out}	1.0 nM	a
Factor IX: z_9^{out}	0.09 μM	a
Factor X: z_{10}^{out}	0.17 μM	a
TFPI: $[TFPI]^{out}$	2.5 nM	d
Platelet: $[PL]^{out}$	$2.5 \cdot 10^5$/mm^3	e
N_2^{pl}	2000	f
N_5^{pl}	3000	g
N_8^{pl}	450	h
N_9^{pl}	250	i
$N_9^{pl,*}$	250	i
N_{10}^{pl}	2700	j

(a) From Mann et al. (1990).
(b) From Mann et al. (1991).
(c) Morrissey (1995) suggests that normal plasma concentration of fVIIa is about 1% of the normal fVII concentration.
(d) From Novotny et al. (1991).
(e) From Weiss (1975).
(f) From Brass et al. (1994).
(g) From Walsh (1994).
(h) From Nesheim et al. (1988).
(i) From Ahmad et al. (1989).
(j) From Mann et al. (1992).

Turitto and coworkers made their measurements. We therefore adjust k_{pla}^+ to $2 \cdot 10^{10}$ M^{-1} s^{-1} so that our model subendothelium is completely covered by platelets in about 5 min. We note that this deposition rate is about threefold slower than that reported in Hubbell and McIntire (1986) for 10 μm by 10 μm regions of a collagen-coated glass surface under similar flow conditions. Note that k_{pla}^+ is the rate constant for adhesion to the surface of platelets that are already in the reaction shell, while k_{flow}^p determines the transport of platelets into the shell.

In the model, three terms contribute to platelet activation, and the rate of change of the activated platelet concentration (both wall-adherent and not) is found by adding Eqs. 48 and 49:

$$\frac{d([PL_a^s] + [PL_a^v])}{dt}$$

$$= \left\{ k_{pla}^+(p_{sub} - [PL_a^s]) + k_{c_2}^{act} \frac{e_2}{e_2^{pla} + e_2} \right.$$

$$\left. + k_{pla}^{act}([PL_a^s] + [PL_a^v]) \right\}[PL]$$

To estimate $k_{e_2}^{act}$, we fit an exponential to the data in Gear (1994) (p. 290) which shows the rate of disappearance of platelet singlets (as doublets and larger platelet clusters form) in a quenched-flow experiment following administration of 10 nM thrombin. The calculated time constant of 0.34 s^{-1} estimates the rate of singlet disappearance at a thrombin concentration of 10 nM. We estimate e_2^{pla} as roughly 1 nM, and equating our expression for the rate of thrombin-induced activation (with $e_2 = 10$ nM and $e_2^{pla} = 1$ nM) to this calculated rate, we infer that $k_{e_2}^{act} = 0.37$ s^{-1}. This value underestimates somewhat the rate of maximal platelet activation by this thrombin concentration, since only a fraction of activated platelets collide and form doublets during Gear's experiment. We estimate the maximal rate of thrombin-induced activation as about 0.5–1.0 s^{-1}. Gear (1994) also gives the maximum rate of ADP-induced singlet disappearance as 0.34 s^{-1} with the half-maximal rate corresponding to an ADP concentration of about 2 μM. Hubbell and McIntire (1986) estimate the average ADP concentration around a small thrombus to be between 0.3 and 0.8 μM depending on shear rate, and this gives a rate of singlet disappearance between .05 and 0.1 s^{-1}. The corresponding rate in the equation above is $k_{pla}^{act}([PL_a^s] + [PL_a^v])$. Noting that $[PL_a^s]$ can be as high as $p_{sub} = 2.2 \cdot 10^{-10}$ M, and that $[PL_a^s] + [PL_a^v]$ can be somewhat higher than this, we estimate k_{pla}^{act} as about $3 \cdot 10^8$ M^{-1} s^{-1} to give an activation rate in the middle of the range 0.05 to 0.1 s^{-1}. With these estimates for $k_{e_2}^{act}$ and k_{pla}^{act}, and with k_{pla}^+ determined as described above, activation of platelets occurs predominantly through contact with the subendothelium during the first 240 s of our simulations, after which time activation by thrombin predominates.

The variables in the model are volume concentrations. We convert surface densities into volume concentrations as follows: For TF and its complexes on the subendothelium, the surface density (e.g., fmol/cm^2) is converted into a concentration by dividing it by the height $\bar{h}$ of the shell. To determine the volume concentrations of platelet-surface binding sites,

we multiply the relevant platelet concentration by the number of binding sites per platelet, so, for example, $p_9 = N_9^{pl}([PL_a^s] + [PL_a^v])$.

In order to compute numerical solutions of the model equations, we first nondimensionalize the equations, which has the effect of tremendously reducing the range of values taken on by model variables. To solve the nondimensionalized equations, we use methods for stiff ordinary differential equations implemented in the software package LSODE (Hindmarsh, 1983). We performed careful convergence studies, varying the numerical time step, to ensure the accuracy of our numerical solutions. A single 10-min simulation takes about 38 s on a SUN Ultra 60 workstation (Sun Microsystems, Palo Alto, CA).

RESULTS

In this section, we present results of computational experiments exploring the behavior of the model system developed in the previous section. Unless indicated otherwise, the parameter values used are those listed in Tables 1–7 and we refer to these, for brevity, as standard values.

Dependence on surface binding site densities

Motivated by our analysis (Fogelson and Kuharsky, 1998) of a simple zymogen/enzyme system which showed the importance of the density of membrane binding sites in controlling the system's responsiveness, we conducted a series of computational experiments differing from one another only in the prescribed density of TF, and we computed the resulting thrombin production. We did this for each of several shear rates. The results are shown in Fig. 4 *a* and indicate that a small change in TF density can induce an increase of thrombin concentration of between three and four orders of magnitude. The thrombin concentrations achieved at densities just above threshold are greater than 1 nM, a concentration at which thrombin has profound effects on platelets (Hubbell and McIntire, 1986). These results show that TF density functions as a switch for the model's overall response.
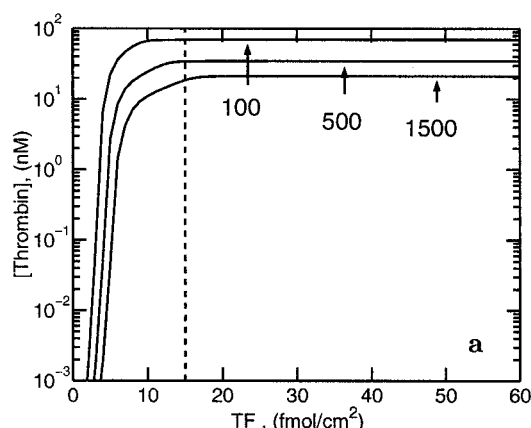
In Fig. 4 *b*, we show results of a different kind of binding-site-density experiment. For these experiments, the TF density was kept fixed at a value of 15 fmol/cm^2 which from Fig. 4 *a* we see is above threshold for all shear rates between 100 and 1500 s^{-1}, and the density of binding sites on the surfaces of activated platelets was varied. For each experiment, the standard values of platelet binding site numbers (e.g., N_9^{pl}) were multiplied by a common factor, and we looked at the resulting thrombin concentration as a function of this multiplier. As Fig. 4 *b* shows, there is again a very steep increase in response as the multiplier is increased from about 0.5 to 1.0 (which corresponds, for example, to a change in fV binding site number from 1500 to 3000 per platelet). This behavior is seen at all shear rates examined. It is interesting to note that the standard values of platelet binding site densities are just above the computed threshold levels.

Dependence on flow shear rate

Fig. 5 *a* shows the time course of thrombin concentration at several shear rates for a TF density of 15 fmol/cm^2 and for standard values of all parameters. We see that for all shear rates in the range 100 to 1500 s^{-1}, the thrombin concentration remains low for 3–5 min, and then increases rapidly over a time interval of about 40–50 s (for example, the interval between 220 and 270 s at shear rate 100 s^{-1}) and reaches a level of 18–70 nM within 600 s. The thrombin concentrations reached at 600 s increase as the shear rate is decreased in this range. Fig. 5 *b* shows that thrombin levels for a TF density of 1 fmol/cm^2 remain very low and decay slowly.

Hemophilias A and B

These are clinical bleeding disorders associated with deficient quantities of factors VIII and IX, respectively. Our
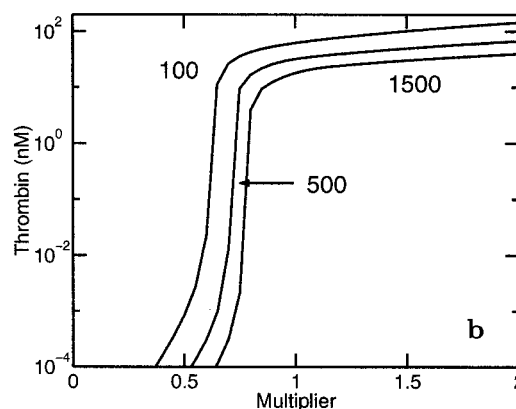

FIGURE 4   Dependence of thrombin concentration at 600 s on (*a*) the density of TF on the subendothelium at shear rates of 100, 500, and 1500 s^{-1}, (*b*) the densities of binding sites on platelets. The value Multiplier = 1 corresponds to the standard values of these densities.
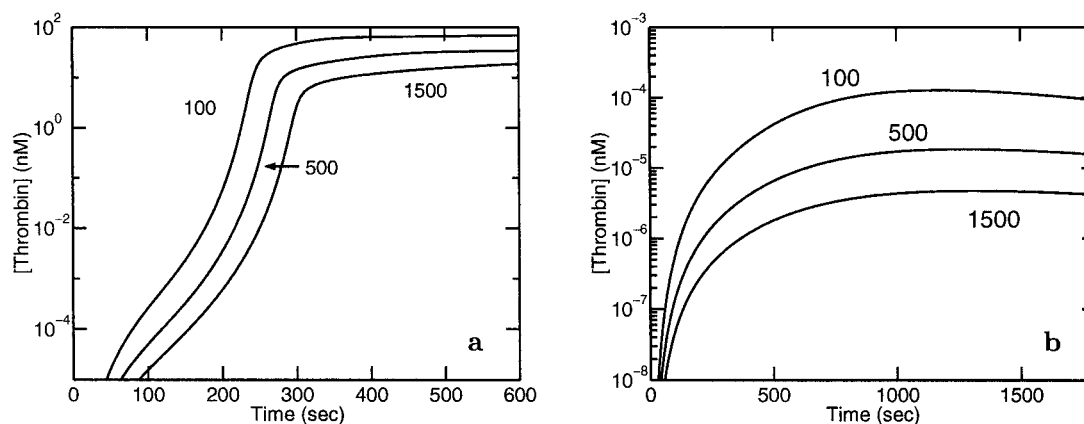
FIGURE 5 Time course of thrombin concentration for shear rates of 100, 500, and 1500 s^{-1} for TF density (*a*) 15 fmol/cm^2 and (*b*) 1 fmol/cm^2. Note different scales.

first attempts to simulate these disorders failed, and we determined that this was due to continued significant production of fXa by the TF:VIIa complex on the subendothelium. As we explain further below, the chemical inhibitor thought to be responsible for shutting off the TF:VIIa complex, namely TFPI:Xa, is present in concentrations far too small to actually accomplish this. It was these observations which led us to add to the model the possibility that platelet deposition on the subendothelium physically inhibits the activity of the TF:VIIa complex.

In Fig. 6, we show results of model simulations with and without the physical inhibition of TF:VIIa by wall-adherent platelets, for a TF density of 15 fmol/cm^2 and standard parameter values. Fig. 6, *a–c*, depicts results with physical inhibition of TF:VIIa and shows significant reductions in thrombin concentration for both hemophilia A and hemo-

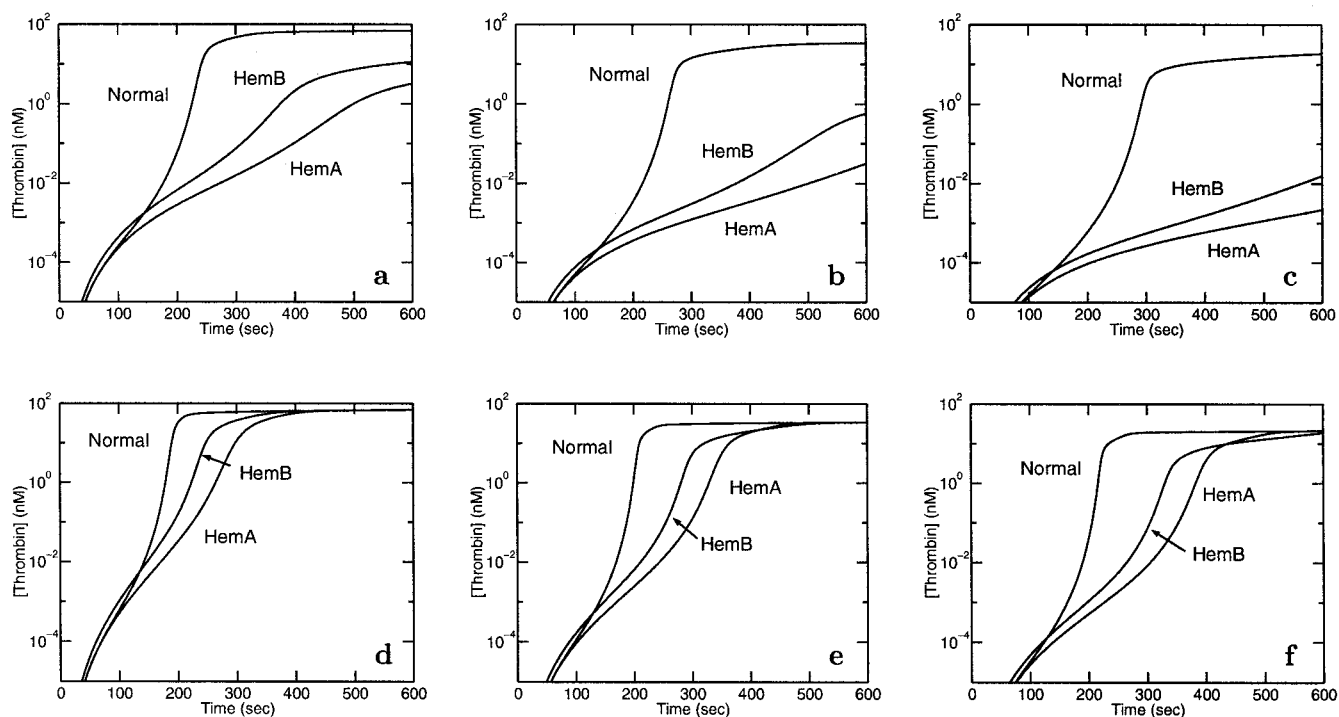FIGURE 6 Hemophilia. Time course of thrombin concentration for different levels of fVIII and fIX and different shear rates and TF density 15 fmol/cm^2. Normal denotes normal levels of fVIII and IX. HemA denotes 1% of normal fVIII and normal fIX. HemB denotes 1% of normal fIX and normal fVIII. Frames (*a*) 100 s^{-1}, (*b*) 500 s^{-1}, and (*c*) 1500 s^{-1} are for simulations in which platelet deposition blocks TF:VIIa activity. Frames (*d*) 100 s^{-1}, (*e*) 500 s^{-1}, and (*f*) 1500 s^{-1} are for simulations in which platelet deposition does not block TF:VIIa activity.

philia B at various shear rates. The degree of reduction increases substantially with increasing shear rate. In each case the reduction for hemophilia A (fVIII deficiency) is more pronounced than for hemophilia B, in agreement with clinical observations. Fig. 6, *d–f*, depicts results without physical inhibition and shows that, in this case, a 100-fold reduction in fVIII or fIX leads to virtually no reduction in thrombin concentration after 600 sec.

Fig. 7 shows the time course of different platelet and enzyme concentrations under normal conditions with physical inhibition of TF:VIIa activity. In Fig. 7 *a*, we see that the concentration of platelets adherent to the subendothelium, $[PL_a^s]$, increases until complete surface coverage is achieved at about 300–350 s. The concentration of activated but not wall-adherent platelets, $[PL_a^v]$, increases more gradually, and, while it is still rising after 600 s, at that time most of the activated platelets are directly adherent to the suben-

dothelium, i.e., the platelets form an approximate monolayer. The concentration of unactivated platelets $[PL]$ initially drops due to activation of platelets (primarily by contact with the subendothelium) and then climbs back to its plasma value.

Fig. 7 *b* shows the decrease of exposed TF molecules as platelets deposit on the subendothelium, and the initial rise and then decline of TF:VII complexes. Note that after about 20 s, most of the exposed TF is bound by fVII. The inset shows semilog plots of the densities of the TF:VII, TF:VIIa, and TF:VIIa:TFPI:Xa complexes. The TF:VIIa density remains roughly 1% of the TF:VII density, and decreases, at first gradually and then sharply coincident with the coverage of subendothelium by platelets. Very little of the decrease can be attributed to inhibition of TF:VIIa by TFPI:Xa as the density of the inhibited TF:VIIa complex (TF:VIIa:TFPI:Xa) remains four orders of magnitude less
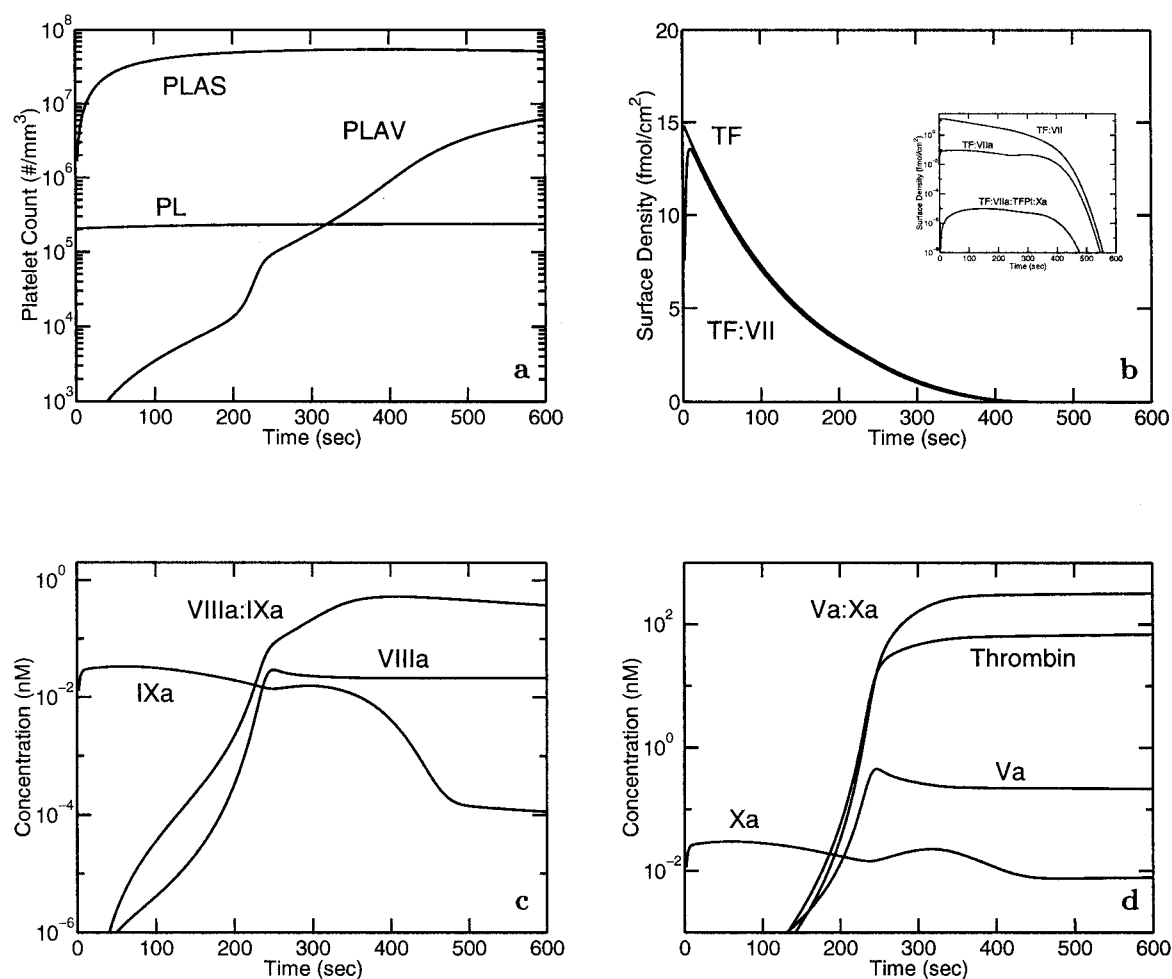

FIGURE 7 Time course of enzyme and platelet concentrations when platelet deposition blocks TF:VIIa activity, standard parameter values are used, the shear rate is 100 s^{-1}, and the TF density is 15 fmol/cm^2. (*a*) Wall-adherent (PLAS), activated (PLAV), and unactivated (PL) platelet concentrations. (*b*) TF (total) and TF:VII densities, and (inset) TF:VII, TF:VIIa, and TF:VIIa:TFPI:Xa densities. (*c*) Plasma fVIIIa and fIXa concentrations and platelet-bound tenase (VIIIa:IXa) complex concentration. (*d*) Plasma fVa, fXa, and thrombin concentrations and platelet-bound prothrombinase (Va:Xa) concentration. Note that PLAS, PLAV, and PL correspond to the model variables $[PL_a^s]$, $[PL_a^v]$, and $[PL]$ but are expressed in plt/mm^3.

than the density of uninhibited TF:VIIa even as the latter decreases. The inhibition of TF:VIIa here is almost completely due to the deposition of platelets on the subendothelium. Fig. 7 c shows that the plasma fVIIIa increases by more than a factor of 10^4, while the plasma fIXa concentration decreases sharply as platelets depositing on the subendothelium cover the TF:VIIa complex that activates IX to IXa. The concentration of the platelet-bound VIIIa:IXa (tenase) complex increases in parallel with the increase of the fVIIIa concentration until the drop in fIXa makes it the limiting species in VIIIa:IXa formation. After this, the concentration of VIIIa:IXa drops, but only slowly because of the high affinity with which it is bound to the platelet surface. Fig. 7d shows that after an initial sharp increase, the plasma fXa concentration varies slowly and over a narrow range during the remainder of the simulation. The concentrations of plasma fV and thrombin and platelet-bound

Va:Xa (prothrombinase) complex increase rapidly between 200 and 240 s and then level off for the remainder of the calculation. Our results are consistent with reports (van't Veer and Mann, 1997) that there are two phases leading up to substantial thrombin production; an initiation phase during which fVa and fVIIIa are becoming available and little thrombin is produced, and a propagation phase in which substantial prothrombinase activity leads to large amounts of thrombin production. Reduction in the level of inhibition (see next paragraph) shortens the length of the initiation phase, as does an increase (not shown) of the TF density to levels well beyond the threshold value. We note that throughout these calculations, zymogen levels in the boundary layer differ only slightly from their initial or upstream values, indicating that reactions are not transport-limited.

Fig. 8 shows results for the case in which platelet deposition does not block TF:VIIa activity. As seen in Fig. 8 a,
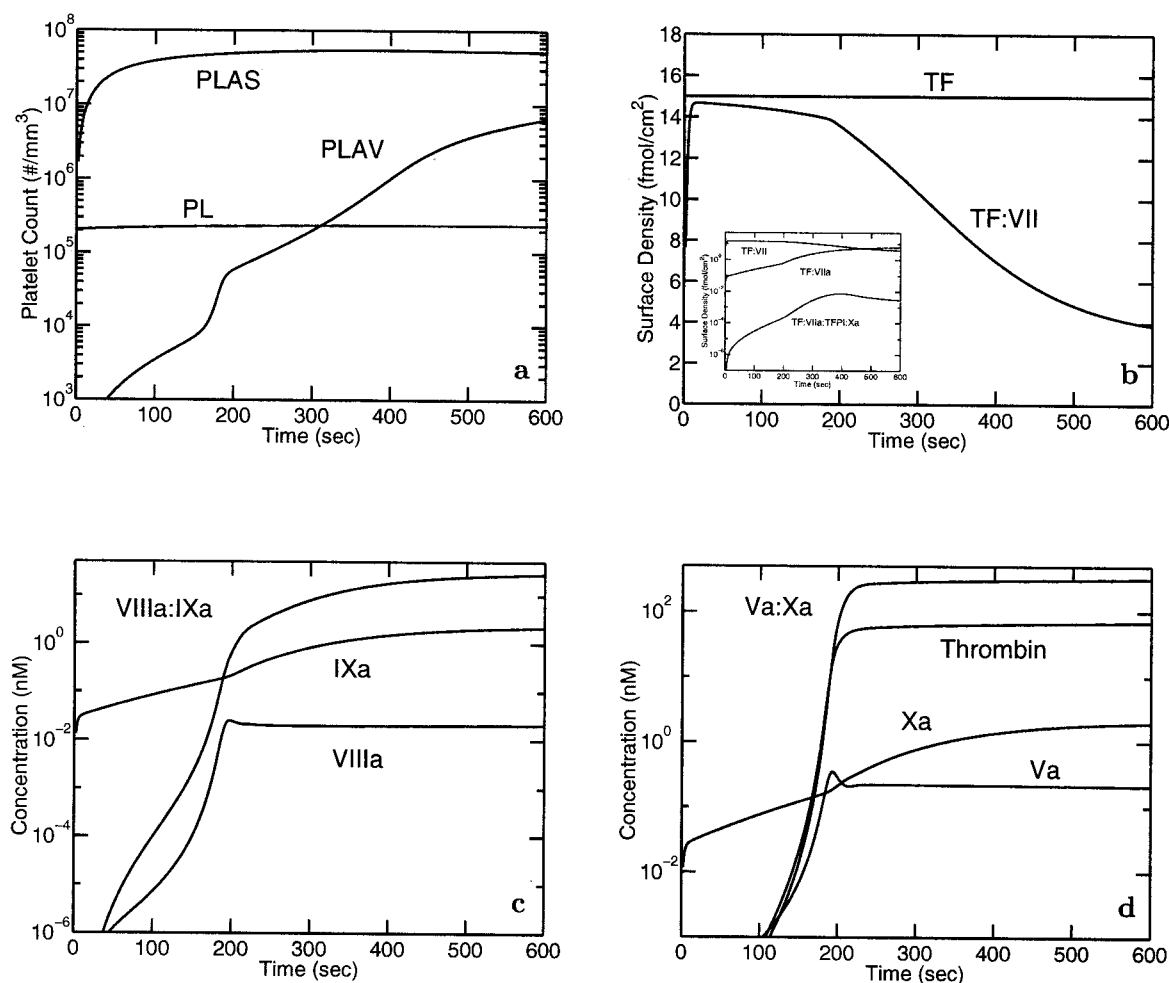

FIGURE 8 Time course of enzyme and platelet concentrations when platelet deposition does not block TF:VIIa activity, standard parameter values are used, the shear rate is 100 s^{-1}, and the TF density is 15 fmol/cm^2. (a) Wall-adherent (PLAS), activated (PLAV), and unactivated (PL) platelet concentrations. (b) TF (total) and TF:VII densities, and (inset) TF:VII, TF:VIIa, and TF:VIIa:TFPI:Xa densities. (c) Plasma fVIIIa and fIXa concentrations and platelet-bound VIIIa:IXa (tenase) complex concentration. (d) Plasma fVa, fXa, and thrombin concentrations and platelet-bound Va:Xa (prothrombinase) concentration.

the evolution of the different platelet populations is very similar to that in Fig. 7 *a*, while Fig. 8 *b* shows that, in contrast, the time course of the TF complexes is very different. The density of exposed TF molecules remains constant throughout the calculation, and the TF:VII density increases sharply as almost all of the TF molecules are bound by fVII, and then decreases fivefold during the remainder of the simulation, due to continuing TF:VII activation. The density of TF:VIIa:TFPI:Xa also continues to increase but is never more than about 1% of the total TF:VIIa density. Thus TFPI:Xa inhibition of TF:VIIa is not effective, the TF:VIIa complex continues to activate fIX and fX throughout the simulation, and the concentrations of fIXa and fXa continue to increase.

Dependence on platelet count

Clinically it is observed (Warkentin and Kelton, 1994) that a decrease in platelet count, thrombocytopenia, by a factor of 10 or more may lead to hemorrhage, with the severity of the problem increasing the smaller the platelet concentration. A decrease in platelet count from 250,000 to 20,000 plt/mm^3 usually does not cause severe enough symptoms for treatment by platelet transfusion (White et al., 1994). In the experiments depicted in Fig. 9, the effect of variations in platelet count on model results is examined at shear rate 500 s^{-1} and TF density of 15 fmol/cm^2. Results for shear rate 100 and 1500 s^{-1} are similar.

Fig. 9 *a* shows that the normal sharp rise in thrombin concentration is delayed by about 100 sec for 10% of normal platelet count (NPC), and that for 1% NPC, the thrombin concentration remains substantially below normal. Fig. 9 *b* shows that for NPC about 90% of the subendothelium is covered by adherent platelets in about 300 s and almost 100% is covered within 400 s. With platelet count 10% of normal, platelet coverage after 600 s is only 40%, and for 1% NPC, the subendothelium is only sparsely covered (<7%) after 600 s. Reflecting the model's physical inhibition of subendothelial-bound complexes, the concentration of TF:VIIa drops sharply for NPC (see Fig. 9 *c*), but continues to rise gradually for platelet counts 10% or 1% of normal as new activation of TF:VII outpaces the slower rate of physical inhibition of TF:VIIa because of slower subendothelial coverage by adherent platelets.

Fig. 9, *d* and *e*, shows that the tenase concentration for 10% NPC eventually exceeds that for NPC, and that the prothrombinase concentrations in the two cases plateau at the same level. For 1% NPC, although the concentrations of these complexes are still rising after 10 min, they remain two to four orders of magnitude below the corresponding concentrations in the NPC and 10% NPC cases. We note also that the rate of fIXa and fXa binding to platelets from the plasma was much smaller than the rate at which these enzymes were produced by TF:VIIa, most of the TF:VIIa-activated fIXa and fXa was removed by the flow, and that the rate of production of fXa on platelets by tenase was substantially higher than the rate of binding of fXa to platelets from plasma (except at 1% NPC).

Dependence on surface reactivity

As mentioned above, (Hubbell and McIntire, 1986) reported threefold faster platelet deposition on a collagen-coated glass surface than that we extrapolated from studies on subendothelium. It is likely that severe vascular injury exposes surfaces that are more platelet-reactive (Badimon et al., 1988; Mailhac et al., 1994) than the matrix exposed in typical subendothelial studies (Turitto and Baumgartner, 1979) and for which Hubbell's data might be more representative. For this reason, we performed simulations differing from those described above only in that the rate of platelet reaction with the wall, k_{pla}^+, was taken to be 10-fold larger, which leads to about threefold faster coverage of the surface. For brevity, we refer to these simulations as fast-surface experiments and the ones above as standard-surface experiments. Notable differences in results are that for the fast-surface experiments a much higher TF density is required to elicit a strong response (compare Fig. 10 *a* with
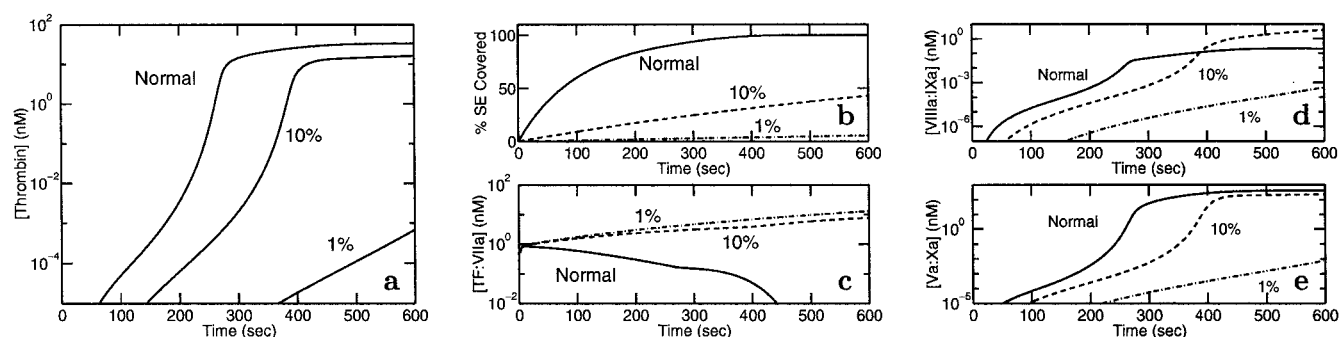

FIGURE 9   Time course of various concentrations for normal platelet count (250,000 plt/mm^3), 10% of normal, and 1% of normal at shear rate 500 s^{-1} and TF density of 15 fmol/cm^2. (*a*) Thrombin concentration. (*b*) Percent of subendothelium covered by platelets. (*c*) TF:VIIa concentration. (*d*) Concentration of tenase VIIIa:IXa on platelets. (*e*) Concentration of prothrombinase Va:Xa on platelets.
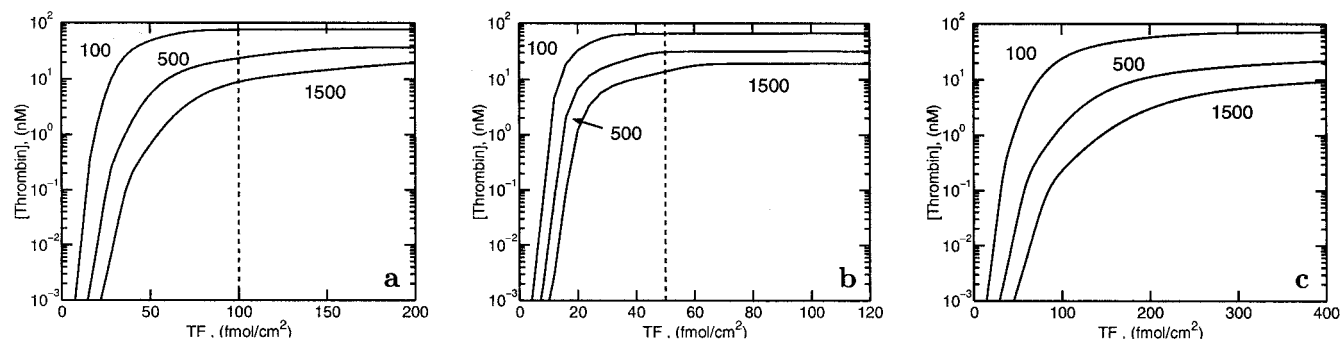
FIGURE 10 Dependence of thrombin concentration at 600 s on the density of TF on the subendothelium at shear rates of 100, 500, and 1500 s^{-1}. (*a*) IXa-specific binding sites and fast-surface. (*b*) Shared IX/IXa binding sites and standard-surface. (*c*) Shared IX/IXa binding sites and fast-surface. Note differences in horizontal scale.

Fig. 4 *a*) and that there is a larger spread between the required TF densities for different shear rates. For the following experiments we used a TF density of 100 fmol/cm^2 to obtain a final thrombin concentration at shear rate 500 s^{-1} the same as that obtained with a TF density of 15 fmol/cm^2 in the standard-surface experiments.

Fig. 11 *a* shows that the system has a response very similar to that for the standard surface when we simulate hemophilia A or B by reducing fVIII or fIX, respectively, to 1% of its normal value. This is for the case that platelet deposition physically inhibits the activity of subendothelial complexes. In the case (not shown) without physical inhi-
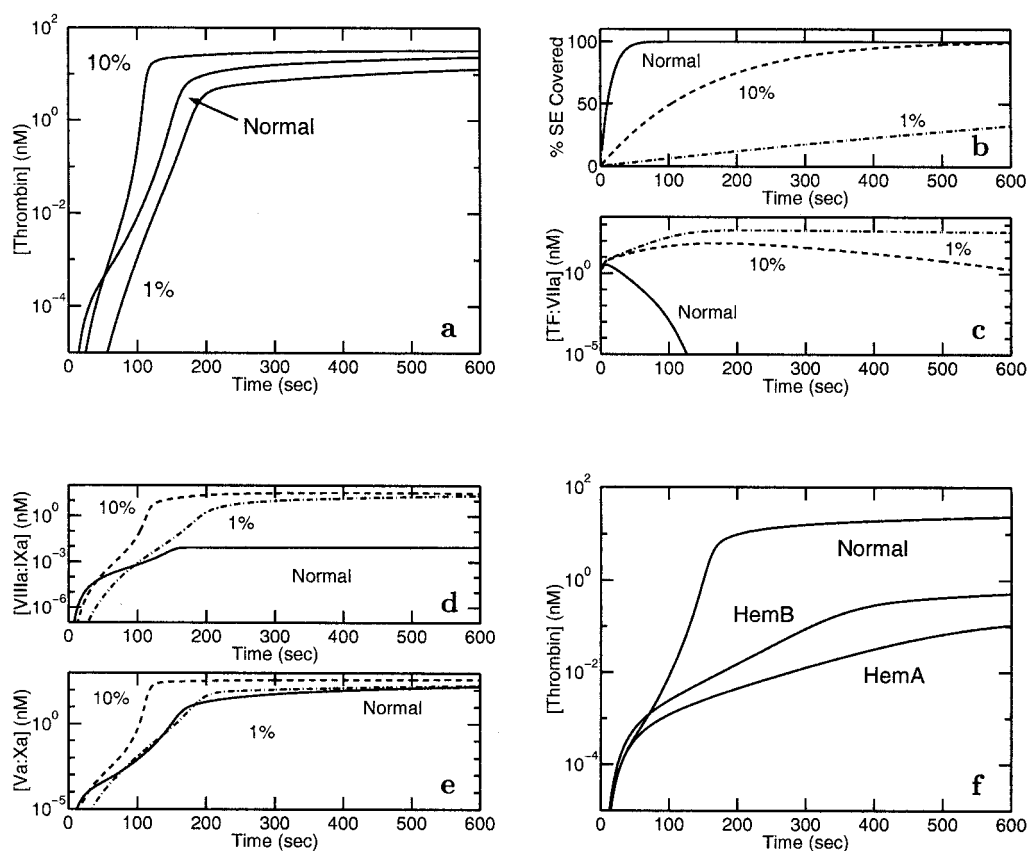

FIGURE 11 Fast surface, shear rate 500 s^{-1}, and TF density of 100 fmol/cm^2. (*a–e*) For normal platelet count (250,000 plt/mm^3), 10% of normal, and 1% of normal, time course of (*a*) Thrombin concentration. (*b*) Percent of subendothelium covered by platelets. (*c*) TF:VIIa concentration. (*d*) Concentration of VIIIa:IXa on platelets. (*e*) Concentration of Va:Xa on platelets. (*f*) For different levels of fVIII and fIX, time course of thrombin concentration. Normal, HemA, and HemB have the same meaning as in Fig. 6.

bition, the thrombin levels for normal blood and for hemophilias A and B are virtually indistinguishable from 200 s until the end of the simulation at 600 s. For the fast surface, time course plots (not shown) for normal blood are similar to those shown in Fig. 7 for the standard surface, except that the increases in the concentrations fVa, fVIIIa, tenase, prothrombinase, and thrombin are sharper and occur earlier, at about 80–100 s compared with 240–270 s.

By contrast, the behavior of the system with the fast surface when the platelet count is reduced is very different from that for the standard surface. Fig. 11 b shows that, for the fast surface, the time course of the thrombin buildup is very similar for all platelet counts, and that the final thrombin concentrations achieved are also very similar, with thrombin concentration slightly higher than normal for the 10% NPC experiment and about half of normal for the 1% NPC experiment. This contrasts with the more than four orders of magnitude reduction of thrombin production with 1% NPC for the standard surface. Fig. 11, b–e, shows the time course of platelet surface coverage and TF:VIIa, VIIIa:IXa and Va:Xa concentrations for this case. These should be compared with Fig. 9, b–e, for the standard surface. Not shown is that, for each platelet count, the activated platelet concentration $[PL_a^s] + [PL_a^v]$ rises much more quickly for the fast surface, so that there are far more activated platelets present at comparable times and at a given platelet count than for the standard surface.

Effect of specific IXa binding sites

To examine the effect of having two populations of fIXa binding sites on platelets, 250 specific IXa sites and 250 shared IX/IXa sites, we performed calculations with 500 shared sites and no specific sites. We drop the terms, underlined in Eqs. 16, 18, 23, and 24, which pertain to the specific sites, and we set N_p^9 to 500. From Fig. 10 b, which shows how thrombin concentration varies with TF density for the standard surface and only shared binding sites, we

see that a much higher TF density, 50 fmol/cm^2, is required to obtain thrombin levels close to those obtained with 15 fmol/cm^2 in calculations with both kinds of IXa binding sites (compare with Fig. 4 a). Similarly, comparison of Fig. 10 c with Fig. 10 a shows it takes a TF density of 400 fmol/cm^2 on the fast surface and with only shared binding sites to reach the same thrombin levels obtained at 100 fmol/cm^2 on that surface with both kinds of IXa binding sites. So for both kinds of surfaces, having only shared IX/IXa binding sites on the platelets leads to a requirement for substantially higher TF densities to elicit substantial thrombin production. Fig. 12 a shows that for normal blood, thrombin develops, at TF 50 fmol/cm^2, much as it does for the two-binding-site case at TF 15 fmol/cm^2. Fig. 12 b shows that thrombin levels are still much reduced for hemophilia A (fVIII deficiency), but are only slightly reduced for the fIX deficiency of hemophilia B.

DISCUSSION

We have formulated a mathematical model of the tissue factor pathway of blood coagulation that takes into account plasma-phase and surface-bound enzymes and zymogens, coagulation inhibitors, and activated and unactivated platelets. It includes both plasma-phase and membrane-phase reactions, and accounts for chemical and cellular transport by flow and diffusion, albeit in a simplified way. Computational studies of the model support three main conclusions: (1) The model system responds in a threshold manner to changes in the availability of particular surface binding sites; an increase in TF binding sites, as would occur with vascular injury, dramatically changes the system's production of thrombin. (2) The model suggests that, at least for small injuries, platelets adhering to and covering the subendothelium, rather than chemical inhibitors, play the dominant role in blocking the activity of the TF:VIIa enzyme complex. And this suggests that a role of the IXa-tenase pathway for activating fX to fXa is to continue fXa produc-
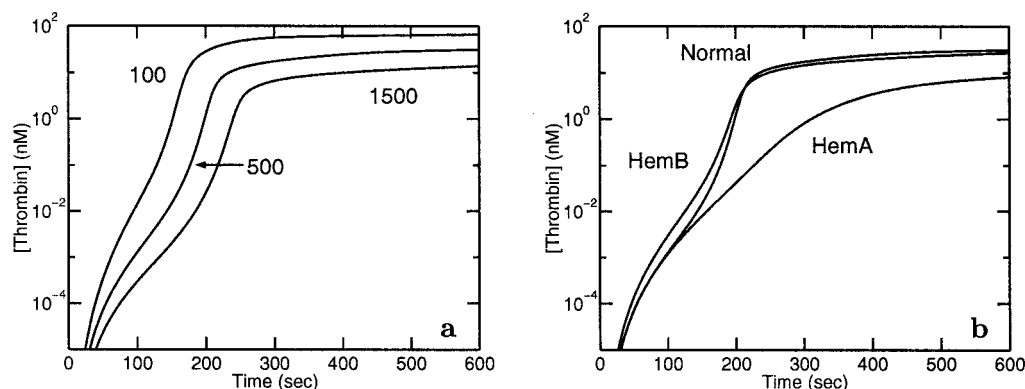

FIGURE 12   Shared IX/IXa binding sites, standard surface, and a TF density of 50 fmol/cm^2. Time course of thrombin concentration for (a) normal blood and various shear rates, (b) different levels of fVIII and fIX and shear rate 500 s^{-1}. Normal, HemA, and HemB have the same meaning as in Fig. 6.

tion after platelets have covered the subendothelial TF:VIIa complexes. (3) The model predicts severely reduced thrombin production for hemophilias A and B, but only if the TF:VIIa activation of fX to fXa has been substantially blocked.

Threshold response

Our results (see Fig. 4 *a*) show a very sharp transition in the model's production of thrombin as the density of TF molecules exposed on the subendothelium is varied; a two- or threefold change in TF density near the transition can induce changes which raise the thrombin concentration by a factor of 10^4. The location of the transition is affected by flow and kinetic parameters, but the existence of the sharp transition is robust over a range of realistic parameter values. Others have found thresholds in models of the coagulation system, but our result is distinct in that the variable (TF density) that controls the threshold is known to change significantly when a vessel is injured. A threshold dependence on TF concentration was recently found in the experimental preparation of van't Veer and Mann (1997).

Activation thresholds that can be adjusted by changes in binding-site densities would be of profound importance to the regulation of coagulation. Blood could normally circulate in a state in which the activation threshold condition is not exceeded, and activated enzyme, say fVIIa, could safely circulate without initiating explosive coagulation. In fact, Morrissey (1995) presents evidence that about 1% of circulating fVII is normally activated. Slight disruptions of the endothelium that exposed small amounts of TF would not lead to coagulation. But a trauma substantial enough to raise the TF levels beyond the transition level would elicit a very strong response, primed by the interaction of the circulating fVIIa with the newly exposed TF. That response would be localized to the immediate vicinity of surfaces on which the binding-site density was high.

Presumably the vasculature is always subject to some degree of localized endothelial disruption and, therefore, to some exposed TF, and this could lead to the coagulation system normally being in an idling state, as suggested in Jesty and Nemerson (1995), in which low levels of thrombin are continually produced. Consistent with this suggestion is the difference between our model's response to a high TF density (15 fmol/cm^2) in which the thrombin concentration reaches 18–70 nM, depending on shear rate, compared to that at a low TF density (1 fmol/cm^2 at shear rate 100 s^{-1}), in which the thrombin concentration reaches a maximum of only $2 \cdot 10^{-4}$ nM after about 1000 s and decays slowly thereafter. In this simulation, platelets cover the exposed subendothelium in about 300–400 s, and then thrombin generation continues because of a low concentration of prothrombinase on the adherent platelets.

Flow serves to bring new zymogens and platelets to the injury and to carry away from it plasma-phase enzymes produced in response to the injury. For the shear rates we examined, the zymogen concentrations in the reaction shell show a transient dip as the simulations start, but soon climb back to near their plasma levels for the remainder of the simulation. The small size of the injury contributes to this; for large areas of injured tissue one would expect zymogen utilization at the upstream portions of the injury to reduce the concentration of zymogen available along the downstream portions. For our simulations, the main effect of higher shear rates is faster removal of plasma-phase enzymes. This has an inhibitory effect on the system causing the threshold level to shift upward at higher shear rate. Flow has a similar role in the explicit threshold condition found for the simpler system studied in Fogelson and Kuharsky (1998). Primarily because of the flow, where an enzyme is produced relative to where it does its work is very important. The effectiveness of fXa made by TF:VIIa is not equal to that of fXa made by the VIIIa:IXa complex, a point also made by Hoffman et al. (1995), in that the former can be washed away by the flow before it can reach the platelet surface, whereas the latter is already where it needs to be to participate in prothrombinase formation.

Our results also show (Fig. 4 *b*) that for high TF levels, the system's response can be further regulated by the densities of platelet binding sites, with a sharp transition in response at densities about half those reported in the literature. These results are preliminary because we changed all platelet binding site densities together and so cannot yet say whether particular types of sites contribute most to this behavior. Even so, these results suggest a certain elegance in platelet design: given the kinetic parameters of the platelet-related enzymes and cofactors (which determine the transition values), the numbers of binding sites per platelet are such that small variations (say 10–20%) in them have a relatively small effect on thrombin production. Therefore, a participating platelet's contribution to the coagulation response is fairly consistent from platelet to platelet. This consistency is achieved with approximately the minimum possible average number of binding sites per platelet; if the average were, say, 75–80% of this number, then platelets with even a slightly below-average number of binding sites would make a greatly reduced contribution to coagulation. Recently, Sumner et al. (1996) found a two- to threefold variation in tenase and prothrombinase activity in the blood of healthy volunteers, which they suggest may be due to variations in specific platelet binding sites. Our simulations suggest that these variations in activity could be accounted for by a 10–20% variation in platelet binding site densities.

In our calculations, the effect of specific platelet binding sites for fIXa is to shift the response threshold to lower TF densities, to sharpen the response as the threshold is crossed, and to reduce the variation between the threshold levels for different shear rates. These can be understood in terms of the relative ease with which any fIXa produced can bind to platelet surfaces, compared to the situation when

fIXa must compete with the more plentiful fIX for shared binding sites. One can regard the presence of specific fIXa binding sites as a way of tuning the coagulation system to be more efficient in its use of fIXa. The body could exploit this efficiency by producing less TF on vascular subsurfaces and still get an adequate response to injury with normal blood. In our calculations with specific IXa binding sites, a TF density of 15 fmol/cm^2 leads to nanomolar or higher thrombin concentrations at all shear rates considered, whereas a TF density of 50 fmol/cm^2 or more is required when only shared IX/IXa binding sites are present. A disadvantage of following this strategy is that the system is then more severely affected when fIX is missing from the system, as in hemophilia B (compare Fig. 6 and Fig. 12 *b*).

Platelet inhibition of TF:VIIa

To our knowledge, the hypothesis that adherent platelets physically inhibit the activity of vessel-bound enzymes like TF:VIIa is new. When our attempts to reproduce the great reduction of thrombin production associated with hemophilia A and B failed, we determined that this failure was due to continued significant production of fXa by the TF:VIIa complex on the subendothelium. This made the alternative pathway to fXa production by the VIIIa:IXa complex on activated platelets superfluous. The main inhibitor of TF:VIIa is regarded to be the plasma protein TFPI; the TFPI molecule must be activated by binding to fXa to become an effective inhibitor of TF:VIIa (Baugh et al., 1998). In our simulations, the concentration of TFPI:Xa was too low to inhibit more than a small percentage of the exposed TF:VIIa molecules. This is the case even though the affinity of binding fXa to TFPI is high ($K_d \approx 2 \cdot 10^{-11}$ M), as is that for the binding of Xa:TFPI to TF:VIIa ($K_d \approx 10^{-10}$ M). In the calculations reported in Fig. 7, which include platelet inhibition of the TF:VIIa complex, the plasma-phase fXa concentration peaked at about 0.03 nM but was generally smaller, and the TFPI:Xa concentration was never more than $2 \cdot 10^{-5}$ nM. In calculations in which platelets do not inhibit TF:VIIa, the fXa concentration reached as high as 1.5 nM (in 600 s), but the TFPI:Xa concentration did not reach 0.02 nM. The concentration of plasma-phase fXa within the reaction shell in our model is very low because of rapid removal of Xa by the flow; its rate of removal by flow almost equals its rate of activation by TF:VIIa. Hence, binding of Xa with TFPI within the reaction shell was strongly limited, and the resulting levels of TFPI:Xa were too low for this complex to compete effectively with fX and fIX in binding to TF:VIIa.

We are certainly not arguing that TFPI plays no inhibitory role in coagulation. The reaction shell in our model is small, covering a 10 μm $\times$ 10 μm square of subendothelium (although similar results were found for squares of side 20 or 40 μm), and flow quickly carries plasma-phase enzymes downstream and out of the shell. The mean time that

a plasma-phase enzyme molecule spends in the shell is about 0.05 s for a shear rate 100 s^{-1} and proportionally less for the higher shear rates. Also, the flow maintains the zymogen level within the shell at approximately its bulk level in the plasma. This combination keeps the concentration of TFPI:Xa low and the concentration of the zymogens with which it competes high. The situation could be different for the downstream section of a long region of exposed subendothelium. Then fX and fIX concentrations near the subendothelium might be depleted because of reactions upstream, and fXa produced upstream could bind to TFPI and inhibit TF:VIIa further downstream. The balance could also be different from that in our simulations in regions of flow recirculation where the zymogen entry rate is reduced and the residence time for locally produced enzyme is higher.

Two recent papers suggest that membrane-associated fXa and TFPI:Xa may be important. Baugh et al. (1998) speculate that fXa remains bound to (or near) the TF:VIIa molecule that activated it, and that TFPI then binds to this ternary complex. This pathway to TFPI:Xa:TF:VIIa formation differs from that previous studies support, and would seem to imply slowed activation of fX because of the continuing presence of fXa bound to TF:VIIa. Salemink et al. (1999) used preformed TFPI:Xa complex, showed that it desorbs slowly from anionic phospholipid membranes, and suggest that subendothelial-bound TFPI:Xa might provide a pool of inhibitor for TF:VIIa that is less subject to removal by flow. They used exogenous TFPI:Xa at concentrations of up to 0.8 nM, which are much higher than those produced in our simulations, and at a TF density, 2.5 fmol/cm^2, lower than the threshold levels found in our simulations. It therefore seems doubtful whether, under the conditions of our current simulations, inclusion of fXa, TFPI, and TFPI:Xa binding to the subendothelium would have a significant effect on our results.

Intuitively, it seems quite plausible that as more platelets adhere to the exposed subendothelium, and thereby cover more and more of the TF:VIIa molecules on it, there are progressively fewer of these molecules available to interact with fX and fIX. We are not aware of any experiments that specifically address this hypothesis. It appears to be consistent with observations made in perfusion studies by Weiss et al. (1986), using blood from a Scott syndrome patient whose platelets aggregated normally but had reduced fXa binding capacity and reduced ability to activate prothrombin in the presence of fVa and fXa and to activate fX in the presence of fVIIIa and fIXa. Whereas for normal blood, Weiss et al. observed an increase in both platelet surface coverage and fibrinopeptide A production (FPA is a by-product of cleavage of fibrinogen into fibrin by thrombin) with increased perfusion time, for Scott syndrome blood, platelet adhesion increased substantially with perfusion time, and this was accompanied by a dramatic decrease in FPA production.

Hemophilias

In the case that adherent platelets block TF:VIIa activity, the model produces results consistent with clinical observations on patients with hemophilias A and B. For both hemophilias, the thrombin concentration is substantially reduced, and the reduction in hemophilia A is more severe than in hemophilia B. We also see (cf. Fig. 6, *a*–*c*) that early in the process, the amount of thrombin produced in hemophilia A is indistinguishable from that produced in normal blood, and that the thrombin concentration in hemophilia B is actually higher than normal. In hemophilia B, the reduced concentration of fIX means that fX has less competition for activation by TF:VIIa, so the early rate of fXa production is higher, and this leads to somewhat greater prothrombinase formation and thrombin production. In normal blood, the activation of fIXa and formation of tenase soon produces enough fXa on the platelet surfaces to overcome this initial lag, but, of course, this does not happen in hemophilia B. We note also that the amount of time before the normal blood thrombin concentration exceeds that in hemophilia B blood decreases with increasing shear rate, and that the severity of the eventual deficit of thrombin production in both hemophilia A and B increases with increasing shear rate. Both observations reflect the fact that fXa activated on the subendothelium must travel through the plasma to bind to platelet surfaces and form prothrombinase. At higher shear rates, more of this fXa is carried downstream before it can bind to platelets. Again, in normal blood, this effect is largely overcome by the production of fXa on the platelet surface by platelet-bound tenase.

Reduced platelet count

The effects of reduced platelet count (thrombocytopenia) for the standard (Fig. 9) and fast (Fig. 11, *a*–*e*) surface illustrate the kinds of balances that influence how much thrombin is produced. They show also that there are two parameters that reflect surface reactivity: the TF density (and associated kinetic parameters) and the rate constant k_{pla}^+ for platelet activation by and adhesion to the surface. For the standard surface at NPC, complete platelet coverage of the surface occurs in about 5 min, and a TF density of 15 fmol/cm^2 is just above threshold. When the platelet count is reduced to 10% or 1% NPC, the surface becomes covered by platelets much more slowly, so TF:VIIa activity continues. On the other hand, the number of activated platelets, along with their pro-coagulant membranes, decreases. For 10% NPC, the continued production of fIXa and fXa by TF:VIIa balances the slower deposition of platelets, and after a delay of about 100 sec, the prothrombinase and thrombin concentrations reach almost their levels for NPC. For 1% NPC, the decreased number of activated platelets is too great, so that despite the continued TF:VIIa activity, the levels of tenase, prothrombinase, and consequently thrombin remain very low. These balances are different on the fast surface where, at NPC, complete surface coverage occurs in about 100 s, and a TF density of 100 fmol/cm^2 is just above threshold. Reduction in platelet count again results in slower surface coverage and continuing TF:VIIa activity. The high TF density leads to fIXa and fXa concentrations that reach peaks 10–100 times larger than those for NPC on the fast surface (and also 10–100 times those at all platelet counts for the standard surface). In this case, the high platelet reactivity of the surface results in rapid activation of platelets (even at reduced platelet counts), thus providing ample surface sites for tenase and prothrombinase formation and consequently high thrombin production. For 10% NPC, the balance among these factors leads to a slightly faster than normal rise in thrombin concentration, whereas for 1% NPC, this rise is slightly slower than normal.

Limitations and extensions

A model with more than 50 differential equations and a corresponding number of kinetic and other parameters is sure to prompt the question of whether essentially any experimental observation could be fit by adjusting parameter values appropriately. This is a reasonable question, and so we wish to emphasize that all kinetic constants and concentrations used in this paper are based on the literature; no fitting was done. When complete kinetic data was not available, we proceeded as described in Model Assumptions above to obtain the parameter values used in this paper. For simulations performed with other values of these parameters that were consistent with literature data, the results were qualitatively similar, but quantitative details such as the threshold level of TF density changed.

The model studied here makes the explicit assumption that chemicals and cells in the reaction region are well mixed, and, based on this, uses a relatively simple model for flow-mediated and diffusive transport. Of course this is a simplification, and it has some consequences. One is that the effective volume concentration of wall-bound chemicals, such as TF, is a function of the flow velocity. This is because the boundary layer thickness depends on flow velocity, and because we have assumed that all cells and chemicals, including those on the vessel wall, are distributed uniformly in the boundary layer. Because the boundary layer thickness depends on the cube-root of velocity, the effective TF volume concentration for any particular TF surface density at shear rate 500 s^{-1} is $5^{1/3} = 1.7$ times that at shear rate 100 s^{-1}, and $3^{-1/3} = 0.7$ times that at shear rate 1500 s^{-1}. These are fairly modest effects, but they make it more difficult to make comparisons between our results at different shear rates. The assumption that things within the boundary layer are well mixed would be a poor one if very slow diffusive transport led to substantial depletion of chemicals or cells in the boundary layer. This does not occur in any situation considered in this paper; in fact, zymogen

levels within the boundary layer are reduced only slightly from their bulk-plasma values. The assumption of well-mixedness becomes suspect for large reaction regions because of the potential effects of upstream zymogen and platelet depletion, and the downstream effect of enzymes produced upstream. The calculations shown in the paper are all for an injury of size 10 μm $\times$ 10 μm, but the fact that similar results were obtained for square injuries of sides 20 and 40 μm, gives us confidence that the results for the smaller injuries are reasonable.

The model studied in this paper is the first we are aware of that combines a fairly comprehensive description of coagulation biochemistry, interactions between platelets and coagulation proteins, explicit treatment of protein binding site densities, and effects of chemical and cellular transport. We think it has potential to give new insights into the dynamics of hemostasis and thrombosis. Still it is limited in assuming spatial homogeneity and in its simple treatment of flow, so we are also working to develop models which allow for spatial heterogeneity, on either a macroscopic (vessel scale) or microscopic (cell scale) level, and which incorporate the effect of realistic multidimensional blood flow and transport. Allowing for realistic flow and spatial heterogeneity requires solving the partial differential equations that govern fluid motion and chemical transport inside of a vessel whose geometry is made complex by the presence of wall-adherent platelets or atherosclerotic plaque. These are very challenging problems whose solution will be facilitated using the computational techniques we have developed for our ongoing studies of the dynamics of platelet aggregation (Fogelson, 1992; Fogelson and Eyre, 1997; Wang and Fogelson, 1999; Yu, 2000). Preliminary work along these lines can be found in Kuharsky (1998).

APPENDIX A

Boundary layer thickness and (k_{flow}^{c}, k_{flow}^{p})

We define the chemical boundary layer as the region from inside of which zymogens and enzymes can reach the exposed subendothelium when it is not covered with activated platelets. To find an estimate of its thickness, we equate the average time it would take a molecule starting at point (x, h) to diffuse to the wall, $h^2/(2D)$, with the time it would take that molecule to be washed past the injured region by the parabolic flow, $(L - x)/V(h)$. Here, h is the molecule's distance from the wall, x is its axial location relative to the upstream end of the injury, L is the length of the injury, D is the

molecular diffusivity, and $V(h) = V \cdot (h/R) \cdot (2 - h/R)$ is the velocity at distance h from the wall when the midstream velocity is V. Solving the equation $(L - x)/V(h) = h^2/2D$ under the assumption that $h \ll 2R$ gives $h(x) = ((L - x) \cdot R \cdot D/V)^{1/3}$. Then, averaging $h(x)$ over the length ($0 \le x \le L$) of the injury gives the average boundary layer thickness:

$$\bar{h} = \frac{3}{4}\left(\frac{R \cdot L \cdot D}{V}\right)^{1/3}.$$

Using this expression, the effective rate of zymogen (enzyme) transport to (from) the shell can be obtained by equating the rate at which the amount of chemical in the layer changes to the rate at which flow brings the chemical across the upstream (downstream) end of the layer:

$$(\bar{h}L \cdot W)\frac{dc}{dt} = \left(2\frac{V}{R}\right)\left(\frac{\bar{h}}{2}\right)(W\bar{h})c.$$

where c is the chemical concentration. Hence,

$$\frac{dc}{dt} = \frac{V \cdot \bar{h}}{R \cdot L}c.$$

So we set k_{flow}^{c} equal to the coefficient of c and arrive at the expression:

$$k_{flow}^{c} = \frac{V \cdot \bar{h}}{R \cdot L}$$

with $\bar{h}$ defined as above.

The parameter k_{flow}^{p} for platelets is defined by a similar expression, except that $\bar{h}$ is replaced by $2 - 3$ μm, the distance at which platelets can attach to other platelets.

Mass transfer coefficients derived in the literature include one found by solving a steady-state advection-diffusion in a short tube with constant concentration along the wall (Baldwin and Basmadjian, 1994; Cussler, 1984):

$$k \approx 0.81\left(\frac{2VD^2}{RL}\right)^{1/3}.$$

This coefficient has dimensions length/time compared with the dimensions time^{-1} for our parameter k_{flow}^{c}. The reason for this difference is that k refers to transport to a surface, while k_{flow}^{c} refers to transport into a volume. To see how the two coefficients are related, we divide k by the average thickness $\bar{h}$ of the boundary layer, and find that

$$k/\bar{h} = 1.81\left[\frac{3}{4}\left(\frac{V^2D}{(RL)^2}\right)^{1/3}\right].$$

Substituting the expression for $\bar{h}$ into the formula for k_{flow}^{c}, we find that

$$k_{flow}^{c} = \left[\frac{3}{4}\left(\frac{V^2D}{(RL)^2}\right)^{1/3}\right]$$

which, except for the constant factor 1.81, is the same as $k/\bar{h}$.

APPENDIX B

Model equations

$$\frac{dz_2}{dt} = -k_2^{on}z_2(p_2 - z_2^{mtot} - e_2^{mtot}) + k_2^{off}z_2^{m} + k_{flow}^{c}(z_2^{out} - z_2) \tag{1}$$

$$\frac{de_2}{dt} = -k_2^{on}e_2(p_2 - z_2^{mtot} - e_2^{mtot}) + k_2^{off}e_2^m + (k_3^- + k_3^{cat})[Z_7^m:E_2] - k_3^+z_7^me_2$$

$$+ (k_{12}^{cat} + k_{12}^-)[Z_5:E_2] - k_{12}^+z_5e_2 + (k_{18}^- + k_{18}^{cat})[Z_7:E_2]$$

$$-k_{18}^+z_7e_2(k_{14}^{cat} + k_{14}^-)[Z_8:E_2] - k_{14}^+z_8e_2 - k_{flow}^ce_2 - k_2^{in}e_2 \tag{2}$$

$$\frac{dz_2^m}{dt} = k_2^{on}z_2(p_2 - z_2^{mtot} - e_2^{mtot}) - k_2^{off}z_2^m - k_7^+z_2^m[PRO] + k_7^-[Z_2^m:PRO] \tag{3}$$

$$\frac{de_2^m}{dt} = k_2^{on}e_2(p_2 - z_2^{mtot} - e_2^{mtot}) - k_2^{off}e_2^m + k_7^{cat}[Z_2^m:PRO]$$

$$+ (k_{13}^{cat} + k_{13}^-)[Z_5^m:E_2^m] - k_{13}^+z_5^me_2^m + (k_{15}^{cat} + k_{15}^-)[Z_8^m:E_2^m] - k_{15}^+z_8^me_2^m \tag{4}$$

$$\frac{dz_5}{dt} = -k_5^{on}z_5(p_5 - z_5^{mtot} - e_5^{mtot}) + k_5^{off}z_5^m - k_{12}^+z_5e_2 + k_{12}^-[Z_5:E_2]$$

$$+ N_5\frac{d([PL_a^s] + [PL_a^v])}{dt} + k_{flow}^c(z_5^{out} - z_5) \tag{5}$$

$$\frac{de_5}{dt} = -k_5^{on}e_5(p_5 - z_5^{mtot} - e_5^{mtot}) + k_5^{off}e_5^m + k_{12}^{cat}[Z_5:E_2] - k_{flow}^ce_5 \tag{6}$$

$$\frac{dz_5^m}{dt} = k_5^{on}z_5(p_5 - z_5^{mtot} - e_5^{mtot}) - k_5^{off}z_5^m - k_5^+z_5^me_{10}^m + k_5^-[Z_5^m:E_{10}^m]$$

$$-k_{13}^+z_5^me_2^m + k_{13}^-[Z_5^m:E_2^m] \tag{7}$$

$$\frac{de_5^m}{dt} = k_5^{on}e_5(p_5 - z_5^{mtot} - e_5^{mtot}) - k_5^{off}e_5^m + k_5^{cat}[Z_5^m:E_{10}^m]$$

$$+ k_{13}^{cat}[Z_5^m:E_2^m] + k_{pro}^-[PRO] - k_{pro}^+e_5^me_{10}^m - k_{16}^+[APC]e_5^m + k_{16}^-[APC:E_5^m] \tag{8}$$

$$\frac{dz_7}{dt} = -k_7^{on}z_7([TF] - e_7^{mtot} - z_7^{mtot}) + k_7^{off}z_7^m - k_1^+z_7e_{10} + k_1^-[Z_7:E_{10}]$$

$$+ k_{18}^-[Z_7:E_2] + k_{flow}^c(z_7^{out} - z_7) \tag{9}$$

$$\frac{de_7}{dt} = -k_7^{on}e_7([TF] - e_7^{mtot} - z_7^{mtot}) + k_7^{off}e_7^m + k_1^{cat}[Z_7:E_{10}]$$

$$+ k_{18}^{cat}[Z_7:E_2] + k_{flow}^c(e_7^{out} - e_7) \tag{10}$$

$$\frac{dz_7^m}{dt} = k_7^{on}z_7([TF] - e_7^{mtot} - z_7^{mtot}) - k_7^{off}z_7^m - k_2^+z_7^me_{10} + k_2^-[Z_7^m:E_{10}]$$

$$-k_3^+z_7^me_2 + k_3^-[Z_7^m:E_2] - z_7^m\frac{p'}{1-p} \tag{11}$$

$$\frac{de_7^m}{dt} = k_7^{on}e_7([TF] - e_7^{mtot} - z_7^{mtot}) - k_7^{off}e_7^m + k_2^{cat}[Z_7^m:E_{10}] + k_3^{cat}[Z_7^m:E_2]$$

$$+ (k_8^- + k_8^{cat})[Z_{10}:E_7^m] - k_8^+z_{10}e_7^m + (k_9^- + k_9^{cat})[Z_9:E_7^m] - k_9^+z_9e_7^m$$

$$-k_{11}^+[TFPI:E_{10}]e_7^m + k_{11}^-[TFPI:E_{10}:E_7^m] - e_7^m\frac{p'}{1-p} \tag{12}$$

$$\frac{dz_8}{dt} = -k_8^{\text{on}} z_8(p_8 - z_8^{\text{mtot}} - e_8^{\text{mtot}}) + k_8^{\text{off}} z_8^{\text{m}} - k_{14}^+ z_8 e_2 + k_{14}^-[Z_8:E_2] + k_{\text{flow}}^{\text{c}}(z_8^{\text{out}} - z_8)$$
(13)

$$\frac{de_8}{dt} = -k_8^{\text{on}} e_8(p_8 - z_8^{\text{mtot}} - e_8^{\text{mtot}}) + k_8^{\text{off}} e_8^{\text{m}} + k_{14}^{\text{cat}}[Z_8:E_2] - k_{\text{flow}}^{\text{c}} e_8$$
(14)

$$\frac{dz_8^{\text{m}}}{dt} = k_8^{\text{on}} z_8(p_8 - z_8^{\text{mtot}} - e_8^{\text{mtot}}) - k_8^{\text{off}} z_8^{\text{m}} - k_6^+ z_8^{\text{m}} e_{10}^{\text{m}} + k_6^-[Z_8^{\text{m}}:E_{10}^{\text{m}}]$$
$$- k_{15}^+ z_8^{\text{m}} e_2^{\text{m}} + k_{15}^-[Z_8^{\text{m}}:E_2^{\text{m}}]$$
(15)

$$\frac{de_8^{\text{m}}}{dt} = k_8^{\text{on}} e_8(p_8 - z_8^{\text{mtot}} - e_8^{\text{mtot}}) - k_8^{\text{off}} e_8^{\text{m}} + k_6^{\text{cat}}[Z_8^{\text{m}}:E_{10}^{\text{m}}] + k_{15}^{\text{cat}}[Z_8^{\text{m}}:E_2^{\text{m}}]$$
$$+ k_{\text{ten}}^-[TEN] - k_{\text{ten}}^+ e_8^{\text{m}} e_9^{\text{m}} - k_{17}^+[APC] e_8^{\text{m}} + k_{17}^-[APC:E_8^{\text{m}}]$$
$$\underline{- k_{\text{ten}}^+ e_8^{\text{m}} e_9^{\text{m},*} + k_{\text{ten}}^-[TEN*]}$$
(16)

$$\frac{dz_9}{dt} = -k_9^{\text{on}} z_9(p_9 - z_9^{\text{mtot}} - e_9^{\text{mtot}}) + k_9^{\text{off}} z_9^{\text{m}} - k_9^+ z_9 e_7^{\text{m}} + k_9^-[Z_9:E_7^{\text{m}}] + k_{\text{flow}}^{\text{c}}(z_9^{\text{out}} - z_9)$$
(17)

$$\frac{de_9}{dt} = -k_9^{\text{on}} e_9(p_9 - z_9^{\text{mtot}} - e_9^{\text{mtot}}) + k_9^{\text{off}} e_9^{\text{m}} + k_9^{\text{cat}}[Z_9:E_7^{\text{m}}] - k_9^{\text{in}} e_9 - k_{\text{flow}}^{\text{c}} e_9$$
$$\underline{- k_9^{\text{on}} e_9(p_9^* - e_9^{\text{m},*} - [TEN*] - [Z_{10}^{\text{m}}:TEN*]) + k_9^{\text{off}} e_9^{\text{m},*}}$$
(18)

$$\frac{dz_9^{\text{m}}}{dt} = k_9^{\text{on}} z_9(p_9 - z_9^{\text{mtot}} - e_9^{\text{mtot}}) - k_9^{\text{off}} z_9^{\text{m}}$$
(19)

$$\frac{de_9^{\text{m}}}{dt} = k_9^{\text{on}} e_9(p_9 - z_9^{\text{mtot}} - e_9^{\text{mtot}}) - k_9^{\text{off}} e_9^{\text{m}} + k_{\text{ten}}^-[TEN] - k_{\text{ten}}^+ e_8^{\text{m}} e_9^{\text{m}}$$
(20)

$$\frac{dz_{10}}{dt} = -k_{10}^{\text{on}} z_{10}(p_{10} - e_{10}^{\text{mtot}} - z_{10}^{\text{mtot}}) + k_{10}^{\text{off}} z_{10}^{\text{m}} - k_8^+ z_{10} e_7^{\text{m}} + k_8^-[Z_{10}:E_7^{\text{m}}] + k_{\text{flow}}^{\text{c}}(z_{10}^{\text{out}} - z_{10})$$
(21)

$$\frac{de_{10}}{dt} = -k_{10}^{\text{on}} e_{10}(p_{10} - e_{10}^{\text{mtot}} - z_{10}^{\text{mtot}}) + k_{10}^{\text{off}} e_{10}^{\text{m}} - k_{10}^+[TFPI] \cdot e_{10} + k_{10}^-[TFPI:E_{10}]$$
$$+ (k_1^- + k_1^{\text{cat}})[Z_7:E_{10}] - k_1^+ z_7 e_{10} + k_8^{\text{cat}}[Z_{10}:E_7^{\text{m}}]$$
$$+ (k_2^- + k_2^{\text{cat}})[Z_7^{\text{m}}:E_{10}] - k_2^+ z_7^{\text{m}} e_{10} - k_{10}^{\text{in}} e_{10} - k_{\text{flow}}^{\text{c}} e_{10}$$
(22)

$$\frac{dz_{10}^{\text{m}}}{dt} = k_{10}^{\text{on}} z_{10}(p_{10} - e_{10}^{\text{mtot}} - z_{10}^{\text{mtot}}) - k_{10}^{\text{off}} z_{10}^{\text{m}} + k_4^-[Z_{10}^{\text{m}}:TEN] - k_4^+ z_{10}^{\text{m}}[TEN]$$
$$\underline{- k_{10}^{\text{on}} z_{10}[TEN*] + k_{10}^{\text{off}}[Z_{10}^{\text{m}}:TEN*]}$$
(23)

$$\frac{de_{10}^{\text{m}}}{dt} = k_{10}^{\text{on}} e_{10}(p_{10} - e_{10}^{\text{mtot}} - z_{10}^{\text{mtot}}) - k_{10}^{\text{off}} e_{10}^{\text{m}} + (k_5^- + k_5^{\text{cat}})[Z_5^{\text{m}}:E_{10}^{\text{m}}] - k_5^+ z_5^{\text{m}} e_{10}^{\text{m}}$$
$$+ (k_6^- + k_6^{\text{cat}})[Z_8^{\text{m}}:E_{10}^{\text{m}}] - k_6^+ z_8^{\text{m}} e_{10}^{\text{m}} + k_{\text{pro}}^-[PRO] - k_{\text{pro}}^+ e_5^{\text{m}} e_{10}^{\text{m}}$$
$$+ k_4^{\text{cat}}[Z_{10}^{\text{m}}:TEN] + \underline{k_4^{\text{cat}}[Z_{10}^{\text{m}}:TEN*]}$$
(24)

$$\frac{d[TEN]}{dt} = k_{\text{ten}}^+ e_8^{\text{m}} e_9^{\text{m}} - k_{\text{ten}}^-[TEN] + (k_4^{\text{cat}} + k_4^-)Z_{10}^{\text{m}}:TEN - k_4^+ z_{10}^{\text{m}}[TEN]$$
(25)

$$\frac{d[PRO]}{dt} = k_{pro}^+ e_5^m e_{10}^m - k_{pro}^-[PRO] + (k_7^{cat} + k_7^-)[Z_2^m:PRO] - k_7^+ z_2^m[PRO] \tag{26}$$

$$\frac{d[Z_2^m:PRO]}{dt} = k_7^+ z_2^m[PRO] - (k_7^- + k_7^{cat})[Z_2^m:PRO] \tag{27}$$

$$\frac{d[Z_5:E_2]}{dt} = k_{12}^+ z_5 e_2 - (k_{12}^- + k_{12}^{cat})[Z_5:E_2] - k_{flow}^c[Z_5:E_2] \tag{28}$$

$$\frac{d[Z_5^m:E_2^m]}{dt} = k_{13}^+ z_5^m e_2^m - (k_{13}^- + k_{13}^{cat})[Z_5^m:E_2^m] \tag{29}$$

$$\frac{d[Z_5^m:E_{10}^m]}{dt} = k_5^+ z_5^m e_{10}^m - (k_5^- + k_5^{cat})[Z_5^m:E_{10}^m] \tag{30}$$

$$\frac{d[Z_7^m:E_2]}{dt} = k_3^+ z_7^m e_2 - (k_3^- + k_3^{cat})[Z_7^m:E_2] - [Z_7^m:E_2]\frac{p'}{1-p} \tag{31}$$

$$\frac{d[Z_7:E_2]}{dt} = k_{18}^+ z_7 e_2 - (k_{18}^- + k_{18}^{cat})[Z_7:E_2] - k_{flow}^c[Z_7:E_2] \tag{32}$$

$$\frac{d[Z_7:E_{10}]}{dt} = k_1^+ z_7 e_{10} - (k_1^- + k_1^{cat})[Z_7:E_{10}] - k_{flow}^c[Z_7:E_{10}] \tag{33}$$

$$\frac{d[Z_7^m:E_{10}]}{dt} = k_2^+ z_7^m e_{10} - (k_2^- + k_2^{cat})[Z_7^m:E_{10}] - [Z_7^m:E_{10}]\frac{p'}{1-p} \tag{34}$$

$$\frac{d[Z_8:E_2]}{dt} = k_{14}^+ z_8 e_2 - (k_{14}^- + k_{14}^{cat})[Z_8:E_2] - k_{flow}^c[Z_8:E_2] \tag{35}$$

$$\frac{d[Z_8^m:E_2^m]}{dt} = k_{15}^+ z_8^m e_2^m - (k_{15}^- + k_{15}^{cat})[Z_8^m:E_2^m] \tag{36}$$

$$\frac{d[Z_8^m:E_{10}^m]}{dt} = k_6^+ z_8^m e_{10}^m - (k_6^- + k_6^{cat})[Z_8^m:E_{10}^m] \tag{37}$$

$$\frac{d[Z_9:E_7^m]}{dt} = k_9^+ z_9 e_7^m - (k_9^- + k_9^{cat})[Z_9:E_7^m] - [Z_9:E_7^m]\frac{p'}{1-p} \tag{38}$$

$$\frac{d[Z_{10}:E_7^m]}{dt} = k_8^+ z_{10} e_7^m - (k_8^- + k_8^{cat})[Z_{10}:E_7^m] - [Z_{10}:E_7^m]\frac{p'}{1-p} \tag{39}$$

$$\frac{d[Z_{10}^m:TEN]}{dt} = k_4^+ z_{10}^m[TEN] - (k_4^- + k_4^{cat})[Z_{10}^m:TEN] \tag{40}$$

$$\frac{d[APC]}{dt} = k_{apc}k_{flow}^c e_2(t - t_{lag}) - k_{16}^+[APC]e_5^m + (k_{16}^- + k_{16}^{cat})[APC:E_5^m]$$

$$- k_{17}^+[APC]e_8^m + (k_{17}^- + k_{17}^{cat})[APC:E_8^m] - k_{flow}^c[APC] \tag{41}$$

$$\frac{d[APC:E_5^m]}{dt} = k_{16}^+[APC]e_5^m - (k_{16}^- + k_{16}^{cat})[APC:E_5^m] \tag{42}$$

$$\frac{d[APC:E_8^m]}{dt} = k_{17}^+[APC]e_8^m - (k_{17}^- + k_{17}^{cat})[APC:E_8^m] \tag{43}$$

$$\frac{d[TFPI]}{dt} = -k_{10}^{+}[TFPI] \cdot e_{10} + k_{10}^{-}[TFPI:E_{10}] + k_{\text{flow}}^{c}([TFPI]^{\text{out}} - [TFPI]) \tag{44}$$

$$\frac{d[TFPI:E_{10}]}{dt} = k_{10}^{+}[TFPI] \cdot e_{10} - k_{10}^{-}[TFPI:E_{10}] + k_{11}^{-}[TFPI:E_{10}:E_{7}^{m}]$$

$$-k_{11}^{+}[TFPI:E_{10}]e_{7}^{m} - k_{\text{flow}}^{c}[TFPI:E_{10}] \tag{45}$$

$$\frac{d[TFPI:E_{10}:E_{7}^{m}]}{dt} = -k_{11}^{-}[TFPI:E_{10}:E_{7}^{m}] + k_{11}^{+}[TFPI:E_{10}]e_{7}^{m} - [TFPI:E_{10}:E_{7}^{m}]\frac{p'}{1-p} \tag{46}$$

$$\frac{d[PL]}{dt} = -k_{\text{pla}}^{+}(p_{\text{sub}} - [PL_{a}^{s}])[PL] - k_{e2}^{\text{act}}[PL]A(e_{2}) - k_{\text{pla}}^{\text{act}}([PL_{a}^{s}] + [PL_{a}^{v}])[PL] - k_{\text{flow}}^{p}([PL]^{\text{out}} - [PL]) \tag{47}$$

$$\frac{d[PL_{a}^{s}]}{dt} = k_{\text{pla}}^{+}(p_{\text{sub}} - [PL_{a}^{s}])([PL] + [PL_{a}^{v}]) - k_{\text{pla}}^{-}[PL_{a}^{s}] \tag{48}$$

$$\frac{d[PL_{a}^{v}]}{dt} = -k_{\text{pla}}^{+}(p_{\text{sub}} - [PL_{a}^{s}])[PL_{a}^{v}] + k_{\text{pla}}^{-}[PL_{a}^{s}] + k_{e2}^{\text{act}}[PL]A(e_{2}) + k_{\text{pla}}^{\text{act}}([PL_{a}^{s}] + [PL_{a}^{v}])[PL] \tag{49}$$

$$\frac{dTF}{dt} = -TF\frac{p'}{1-p} \tag{50}$$

$$\frac{dp_{10}}{dt} = N_{10}^{\text{pl}}\frac{d([PL_{a}^{s}] + [PL_{a}^{v}])}{dt} \tag{51}$$

$$\frac{dp_{5}}{dt} = N_{5}^{\text{pl}}\frac{d([PL_{a}^{s}] + [PL_{a}^{v}])}{dt} \tag{52}$$

$$\frac{dp_{8}}{dt} = N_{8}^{\text{pl}}\frac{d([PL_{a}^{s}] + [PL_{a}^{v}])}{dt} \tag{53}$$

$$\frac{dp_{9}}{dt} = N_{9}^{\text{pl}}\frac{d([PL_{a}^{s}] + [PL_{a}^{v}])}{dt} \tag{54}$$

$$\frac{dp_{2}}{dt} = N_{2}^{\text{pl}}\frac{d([PL_{a}^{s}] + [PL_{a}^{v}])}{dt} \tag{55}$$

$$\frac{de_{9}^{m,*}}{dt} = k_{9}^{\text{on}}e_{9}(p_{9}^{*} - e_{9}^{m,*} - [TEN*] - [Z_{10}^{m}:TEN*]) - k_{9}^{\text{off}}e_{9}^{m,*} + k_{\text{ten}}^{-}[TEN*] - k_{\text{ten}}^{+}e_{8}^{m}e_{9}^{m,*} \tag{56}$$

$$\frac{d[TEN*]}{dt} = k_{\text{ten}}^{+}e_{8}^{m}e_{9}^{m,*} - k_{\text{ten}}^{-}[TEN*] + (k_{4}^{\text{cat}} + k_{4}^{-})[Z_{10}^{m}:TEN*] - k_{4}^{+}z_{10}^{m}[TEN*] \tag{57}$$

$$\frac{d[Z_{10}^{m}:TEN*]}{dt} = k_{4}^{+}z_{10}^{m}[TEN*] - (k_{4}^{-} + k_{4}^{\text{cat}})[Z_{10}^{m}:TEN*] \tag{58}$$

$$\frac{dp_{9}^{*}}{dt} = N_{9}^{\text{pl},*}\frac{d([PL_{a}^{s}] + [PL_{a}^{v}])}{dt} \tag{59}$$

REFERENCES

Ahmad, S., R. Rawala-Sheikh, and P. Walsh. 1989. Comparative interactions of factor IX and factor IXa with human platelets. *J. Biol. Chem.* 264:3244.

Badimon, L., J. J. Badimon, V. T. Turitto, S. Vallabhajosula, and V. Fuster. 1988. Platelet thrombus formation on collagen type I. A model of deep

vessel injury: influence of blood rheology, von Willebrand factor, and blood coagulation. *Circulation.* 78:1431–1442.

Baldwin, S. A., and D. Basmadjian. 1994. A mathematical model of thrombin production in blood coagulation, Part I: The sparsely covered membrane case. *Ann. Biomed. Eng.* 22:357–370.

Bauer, K. A., and R. D. Rosenberg. 1987. The pathophysiology of the prethrombotic state in humans: Insights gained from studies using markers of hemostatic system activation. *Blood.* 70:343–350.

Baugh, R. J., G. J. Broze, and S. Krishnaswamy. 1998. Regulation of extrinsic pathway factor Xa formation by Tissue Factor Pathway Inhibitor. *J. Biol. Chem.* 273:4378–4386.

Beltrami, E., and J. Jesty. 1995. Mathematical analysis of activation thresholds in enzyme-catalyzed positive feedbacks: application to the feedbacks of blood coagulation. *Proc. Natl. Acad. Sci. USA.* 92: 8744–8748.

Brass, L., M. Ahuja, E. Belmonte, S. P. S. A. Tarver, and J. Hoxie. 1994. The human platelet thrombin receptor: turning it on and turning it off. *Ann. N.Y. Acad. Sci.* 714:1–12.

Broze, G., L. A. Warren, W. F. Novotny, D. A. Higuchi, J. J. Girard, and J. Miletich. 1988. The lipoprotein-associated coagulation inhibitor that inhibits the factor VII-tissue factor complex also inhibits factor Xa: insight into its possible mechanism of action. *Blood.* 71:335.

Broze, G. J., T. J. Girard, and W. F. Novotny. 1990. Regulation of coagulation by multi-valent Kunitz-type inhibitor. *Biochemistry.* 29: 7539–7546.

Butenas, S., and K. G. Mann. 1996. Kinetics of human factor VII activation. *Biochemistry.* 35:1904–1910.

Cussler, E. 1984. Diffusion: Mass Transfer in Fluid Systems. Cambridge University Press, Cambridge.

Eaton, D., H. Rodriguez, and G. A. Vehar. 1986. Proteolytic processing of human factor VIII: correlation of specific cleavages by thrombin, factor Xa, and activated protein C with activation and inactivation of factor VIII coagulant activity. *Biochemistry.* 25:505–512.

Esmon, C. T. 1989. The roles of protein C and thrombomodulin in the regulation of blood coagulation. *J. Biol. Chem.* 264:4743–4746.

Fogelson, A. L. 1992. Continuum models of platelet aggregation: formulation and mechanical properties. *SIAM JAM* 52:1089.

Fogelson, A. L., and D. J. Eyre. 1997. IBIS: Immersed Boundary and Interface Software package. http://www.math.utah.edu/IBIS.

Fogelson, A. L., and A. L. Kuharsky. 1998. Membrane binding-site density can modulate activation thresholds in enzyme systems. *J. Theor. Biol.* 193:1–18.

Frojmovic, M. M., K. Longmire, and T. van de Ven. 1990. Long-range interactions in mammalian platelet aggregation. II. The role of platelet pseudopod number and length. *Biophys. J.* 58:309–318.

Gear, A. R. L. 1994. Platelet adhesion, shape change, and aggregation: rapid initiation and signal transduction events. *Can. J. Physiol. Pharmacol.* 72:285–94.

Gemmell, C. H., V. T. Turitto, and Y. Nemerson. 1988. Flow as a regulator of the activation of factor X by tissue factor. *Blood.* 72:1404–1408.

Hemker, H. C., and H. Kessels. 1991. Feedback mechanisms in coagulation. *Haemostasis.* 21:189–196.

Hill-Eubanks, D. C., and P. Lollar. 1990. von Willibrand factor is a cofactor for thrombin-catalyzed cleavage of the factor VIII light chain. *J. Biol. Chem.* 265:17854–17858.

Hindmarsh, A. C. 1983. ODEPACK, a systematized collection of ODE solvers. *In* Scientific Computing. R. S. Stepleman, editor. Volume 1 of *IMACS Transactions on Scientific Computation.* North-Holland, Amsterdam. 55–64.

Hoffman, M., D. Monroe, J. Oliver, and H. Roberts. 1995. Factors IXa and Xa play distinct roles in tissue factor-dependent initiation of coagulation. *Blood.* 86:1794–1801.

Hubbell, J. A., and L. V. McIntire. 1986. Platelet active concentration profiles near growing thrombi: a mathematical consideration. *Biophys. J.* 50:937–945.

Jesty, J., E. Beltrami, and G. Willems. 1993. Mathematical analysis of a proteolytic positive-feedback loop: dependence of lag time and enzyme

yields on the initial conditions and kinetic parameters. *Biochemistry.* 32:6266–6274.

Jesty, J., and Y. Nemerson. 1995. The pathways of blood coagulation. *In* Williams Hematology (5th ed.). E. Beutler, M. Lichtman, and B. Coller, editors. McGraw-Hill, New York. 1227–1238.

Jesty, J., T. Wun, and A. Lorenz. 1994. Kinetics of the inhibition of factor Xa and the tissue factor-factor VIIa complex by the tissue factor pathway inhibitor in the presence and absence of heparin. *Biochemistry.* 33:12686–12694.

Jones, K., and K. G. Mann. 1994. A model for the tissue factor pathway to thrombin. II. A mathematical simulation. *J. Biol. Chem.* 269: 23367–23373.

Krishnaswamy, S., K. A. Field, T. S. Edgington, J. H. Morrissey, and K. G. Mann. 1992. Role of the membrane surface in the activation of human coagulation factor X. *J. Biol. Chem.* 267:26110–26120.

Krishnaswamy, S., K. C. Jones, and K. G. Mann. 1988. Prothrombinase complex assembly: kinetic mechanism of enzyme assembly on phospholipid vesicles. *J. Biol. Chem.* 263:3823–3834.

Krishnaswamy, S., M. Nesheim, E. Pryzdial, and K. G. Mann. 1993. Assembly of the prothrombinase complex. *Methods Enzymol.* 222: 260–280.

Kuharsky, A. 1998. *Mathematical Modeling of Blood Coagulation.* Ph.D. thesis. University of Utah.

Lollar, P., G. J. Knutson, and D. N. Fass. 1985. Activation of porcine factor VIII:C by thrombin and factor Xa. *Biochemistry.* 24:8056–8064.

Mailhac, A., J. J. Badimon, J. Fallon, A. Fernandez-Ortiz, B. Meyer, J. Chesebro, V. Fuster, and L. Badimon. 1994. Effect of an eccentric severe stenosis on fibrin(ogen) deposition on severely damaged vessel wall in arterial thrombosis, relative contribution of fibrin(ogen) and platelets. *Circulation.* 90:988–996.

Mann, K. G. 1987. The assembly of blood clotting complexes on membranes. *Trends Biosci.* 12:229–233.

Mann, K. G. 1994. Prothrombin and thrombin. *In* Hemostasis and Thrombosis: Basic Principles and Clinical Practice, 3d ed. R. Colman, J. Hirsh, V. Marder, and E. Salzman, editors. J.B. Lippincott Company, Philadelphia. 184–199.

Mann, K. G., E. G. Bovill, and S. Krishnaswamy. 1991. Surface-dependent reactions in the propagation phase of blood coagulation. *Ann. N.Y. Acad. Sci.* 614:63–75.

Mann, K. G., S. Krishnaswamy, and J. H. Lawson. 1992. Surface-dependent hemostasis. *Semin. Hematol.* 29:213–226.

Mann, K. G., M. E. Nesheim, W. R. Church, P. Haley, and S. Krishnaswamy. 1990. Surface-dependent reactions of the vitamin K-dependent enzyme complexes. *Blood.* 76:1–16.

Miletich, J. P., C. M. Jackson, and P. W. Majerus. 1977. Interaction of coagulation factor Xa with human platelets. *Proc. Natl. Acad. Sci. USA.* 74:4033–4036.

Monkovic, D. D., and P. B. Tracy. 1990a. Activation of human factor V by factor Xa and thrombin. *Biochemistry.* 29:1118.

Monkovic, D. D., and P. B. Tracy. 1990b. Functional characterization of human platelet-released factor V and its activation by factor Xa and thrombin. *J. Biol. Chem.* 265:17132–17140.

Morrissey, J. H. 1995. Tissue factor modulation of factor VIIa activity: use in measuring trace levels of factor VIIa in plasma. *Thromb. Haemost.* 74:185–188.

Nemerson, Y. 1992. The tissue factor pathway of blood coagulation. *Semin. Hematol.* 29:170–176.

Nesheim, M. E., D. D. Pittman, J. H. Wang, D. Slonosky, A. R. Giles, and R. J. Kaufman. 1988. The binding of s-labeled recombinant factor VIII to activated and unactivated human platelets. *J. Biol. Chem.* 263:16467.

Nesheim, M. E., R. P. Tracy, and K. G. Mann. 1984. 'Clotspeed', a mathematical simulation of the functional properties of prothrombinase. *J. Biol. Chem.* 259:1447–1453.

Nesheim, M. E., R. P. Tracy, P. B. Tracy, D. S. Boskovic, and K. G. Mann. 1992. Mathematical simulation of prothrominase. *Methods Enzymol.* 215:316–328.

Novotny, W. F., S. Brown, J. Miletich, D. Rader, and G. Broze. 1991. Plasma antigen levels of the lipoprotein-associated coagulation inhibitor in patient samples. *Blood.* 78:387–393.

Radcliffe, R., and Y. Nemerson. 1975. Activation and control of factor VII by activated factor X and thrombin. Isolation and characterization of a single chain form of factor VII. *J. Biol. Chem.* 250:388.

Radcliffe, R., and Y. Nemerson. 1976. Mechanism of activation of bovine factor VII: products of cleavage by factor Xa. *J. Biol. Chem.* 251:4797–4802.

Rao, L. V., and S. I. Rapaport. 1988. Activation of factor VII bound to tissue factor: a key early step in the tissue factor pathway of blood coagulation. *Proc. Natl. Acad. Sci. USA.* 85:6687.

Rapaport, S. 1989. Inhibition of factor VIIa/tissue factor induced blood coagulation: with particular emphasis upon a factor Xa-dependent inhibitory mechanism. *Blood.* 73:359–365.

Rawala-Sheikh, R., S. Ahmad, B. Ashby, and P. Walsh. 1990. Kinetics of coagulation factor X activation by platelet-bound factor IXa. *Biochemistry.* 29:2606–2611.

Rosenberg, R., and K. Bauer. 1994. The heparin-antithrombin system: A natural anticoagulant mechanism. *In* Hemostasis and Thrombosis: Basic Principles and Clinical Practice, 3d ed. R. Colman, J. Hirsh, V. Marder, and E. Salzman, editors. J.B. Lippincott Company, Philadelphia. 837–860.

Rosing, J., G. Tans, W. G.-R. WP, R. Zwaal, and H. C. Hemker. 1980. The role of phospholipids and factor Va in the prothrombinase complex. *J. Biol. Chem.* 255:274–283.

Salemink, I., J. Franssen, G. Willens, and H. C. Hemker. 1999. Inhibition of tissue factor-factor VIIa-catalyzed factor X activation by factor Xa-tissue factor pathway inhibitor. *J. Biol. Chem.* 274:28225–28232.

Silverberg, S., Y. Nemerson, and M. Zur. 1977. Kinetics of the activation of bovine coagulation Factor X by components of the extrinsic pathway. *J. Biol. Chem.* 252:8481–8488.

Solymoss, S., M. M. Tucker, and P. B. Tracy. 1988. Kinetics of inactivation of membrane-bound factor Va by activated protein C: protein S modulates factor Xa protection. *J. Biol. Chem.* 263:14884–14890.

Sumner, W. T., D. M. Monroe, and M. Hoffman. 1996. Variability in platelet procoagulant activity in healthy volunteers. *Thromb. Res.* 81:533–543.

Turitto, V., and H. Baumgartner. 1979. Platelet interaction with subendothelium in flowing rabbit blood: effect of blood shear rate. *Microvasc. Res.* 17:38–54.

Turitto, V., H. Weiss, and H. Baumgartner. 1980. The effect of shear rate on platelet interaction with subendothelium exposed to citrated human blood. *Microvasc. Res.* 19:352–365.

van't Veer, C., and K. G. Mann. 1997. Regulation of tissue factor initiated thrombin generation by the stoichiometric inhibitors tissue factor pathway inhibitor, antithrombin-III, and heparin cofactor-II. *J. Biol. Chem.* 272:4367–4377.

Vehar, G. A., and E. W. Davie. 1980. Preparations and properties of bovine factor VIII (antihemophilic Factor). *Biochemistry.* 19:401.

Walker, F. J., S. I. Chavin, and P. Fay. 1987. Inactivation of factor VIII by activated protein C and protein S. *Arch. Biochem. Biophys.* 252:322.

Walsh, P. N. 1994. Platelet-coagulant protein interactions. *In* Hemostasis and Thrombosis: Basic Principles and Clinical Practice, 3d ed. R. Colman, J. Hirsh, V. Marder, and E. Salzman, editors. J.B. Lippincott Company, Philadelphia. 629–651.

Wang, N. T., and A. L. Fogelson. 1999. Computational methods for continuum models of platelet aggregation. *J. Comput. Phys.* 151:649–675.

Warkentin, T., and J. Kelton. 1994. Management of thrombocytopenia. *In* Hemostasis and Thrombosis: Basic Principles and Clinical Practice, 3rd ed. R. Colman, J. Hirsh, V. Marder, and E. Salzman, editors. J.B. Lippincott Company, Philadelphia. 469–488.

Weiss, H. 1975. Platelet physiology and abnormalities of platelet function (part 1). *New Engl. J. Med.* 293:531–541.

Weiss, H. J., V. T. Turitto, and H. R. Baumgartner. 1986. Role of shear rate and platelets in promoting fibrin formation on rabbit subendothelium, studies utilizing patients with quantitative and qualitative platelet defects. *J. Clin. Invest.* 78:1072–1082.

White, G., V. J. Marder, R. C. Colman, J. Hirsh, and E. Salzman. 1994. Approach to the bleeding patient. *In* Hemostasis and Thrombosis: Basic Principles and Clinical Practice, 3d ed. R. Colman, J. Hirsh, V. Marder, and E. Salzman, editors. J.B. Lippincott Company, Philadelphia. 1134–1147.

Willems, G. M., T. Lindhout, W. T. Hermens, and H. C. Hemker. 1991. Simulation model for thrombin generation in plasma. *Haemostasis.* 21:197–207.

Yu, H. 2000. *Three-Dimensional Computational Modeling and Simulation of Platelet Aggregation on Parallel Computers.* Ph.D. thesis. University of Utah.

Zur, M., and Y. Nemerson. 1980. Kinetics of factor IX activation via the extrinsic pathway. *J. Biol. Chem.* 255:5703–5707.